NASA Technical Paper 1431

Effects of Primary Rotor Parameters on Flapping Dynamics

Robert T. N. Chen

JANUARY 1980

NASA

NASA Technical Paper 1431

Effects of Primary Rotor Parameters on Flapping Dynamics

Robert T. N. Chen
Ames Research Center
Moffett Field, California

National Aeronautics
and Space Administration

**Scientific and Technical
Information Office**

1980

NOMENCLATURE

a blade lift-curve slope

a_0 blade coning angle measured from hub plane, rad (or deg)

a_1 longitudinal first-harmonic flapping coefficient measured from hub plane and in wind-hub system, rad (or deg)

a_{1s} longitudinal first-harmonic flapping coefficient measured from hub plane and in hub-body system, rad (or deg)

A_{1c} lateral cyclic pitch measured from hub plane and in wind-hub system, rad (or deg)

A_{1s} lateral cyclic pitch measured from hub plane and in hub-body system, rad (or deg)

b_1 lateral first-harmonic flapping coefficient measured from hub plane and in wind-hub system, rad (or deg)

b_{1s} lateral first-harmonic flapping coefficient measured from hub plane and in hub-body system, rad (or deg)

B_{1c} longitudinal cyclic pitch measured from hub plane and in wind-hub system, rad (or deg)

B_{1s} longitudinal cyclic pitch measured from hub plane and in hub-body system, rad (or deg)

c blade chord, m

e flapping hinge offset, m

I_β blade moment of inertia about flapping hinge, kg-m^2

K_1 pitch-flap coupling ratio, $\triangleq \tan \delta_3$

K_β flapping hinge restraint, N-m/rad

M_β blade mass moment about the flapping hinge, kg-m

N number of blade

p aircraft roll rate in hub-body system, rad/sec

$\dot{p}$ aircraft roll acceleration, rad/sec^2

p_w aircraft roll rate in wind-hub system, rad/sec, $p_w = p \cos \beta_w + q \sin \beta_w$

P	ratio of flapping frequency to rotor system angular velocity
q	aircraft pitch rate in hub-body system, rad/sec
$\dot{q}$	aircraft pitch acceleration, rad/sec^2
q_w	aircraft pitch rate in wind-hub system, rad/sec, $q_w = -p \sin \beta_w + q \cos \beta_w$
r'	radial station of the blade element measured from the flapping hinge, m
R	rotor radius, m
v_i	uniform induced velocity, m/sec
V	true airspeed, m/sec
x	nondimensional radial station of the blade element, $x \triangleq \frac{e + r'}{R}$
x_s, y_s, z_s	wind-hub system
x'_s, y'_s, z'_s	hub-body system
α	hub plane angle of attack, deg
β	blade flapping angle measured from hub plane, rad (or deg)
$\dot{\beta}$	derivative of flapping with respect to time, $\beta \triangleq \frac{d\beta}{dt}$
$\ddot{\beta}$	second derivative of flapping with respect to time, $\ddot{\beta} \triangleq \frac{d^2\beta}{dt^2}$
β_d	differential collective flapping (only for even-bladed rotors)
β_{nc}	nth order longitudinal cyclic flapping
β_{ns}	nth order lateral cyclic flapping
β_0	collective flapping (coning)
$\beta_0, \beta_d, \beta_{1c}, \beta_{1s}, \ldots, \beta_{nc}, \beta_{ns}$	multiblade flapping coordinates

β_w rotor sideslip angle, that is, the angle between x_s and x_s', deg

γ Lock number, $\triangleq \frac{\rho a c R^4}{I_\beta}$

δ_A lateral control displacement, cm

δ_L longitudinal control displacement, cm

ϵ $\frac{e}{R}$

θ blade pitch angle measured from hub plane,
$\theta = \theta_0 - A_{1c} \cos \psi - B_{1c} \sin \psi + K\theta_t - K_1\beta$, rad (or deg)

ζ damping ratio

θ_0 blade-root collective pitch measured from hub plane, rad (or deg)

θ_t total blade twist (tip with respect to root), deg

λ inflow ratio, $\frac{V \sin \alpha - v_i}{\Omega R}$

μ advance ratio, $\frac{V \cos \alpha}{\Omega R}$

ρ air density, kg/m^3

σ rotor solidity ratio

ϕ control advance angle, deg

ψ azimuth angle measured from downwind in the sense of rotor rotation, rad (or deg)

ψ' azimuth angle measured from $-x_s'$ in the sense of rotor rotation, rad (or deg)

ω_n undamped natural frequency, rad/sec

Ω rotor system angular velocity, rad/sec

Subscript

s.s. steady state

EFFECTS OF PRIMARY ROTOR PARAMETERS ON FLAPPING DYNAMICS

Robert T. N. Chen

Ames Research Center

SUMMARY

An analysis has been made to study the effects of flapping dynamics of four main rotor design features that influence the agility, stability, and operational safety of helicopters. The parameters include flapping hinge offset, flapping hinge restraint, pitch-flap coupling, and blade Lock number. First, the flapping equations of motion are derived that explicitly contain the design parameters. The dynamic equations are then developed for the tip-path plane, and the influence of individual and combined variations in the design parameters determined.

The analysis includes a study of the steady-state flapping response with respect to control input and aircraft angular rate which leads to a feedforward control law for control decoupling through cross feed, and a feedback control law to decouple the steady-state flapping response. The condition for achieving perfect decoupling of the flapping response due to aircraft pitch and roll rates without using feedback control is also found for the hover case.

The analysis also indicates that the frequency of the regressing flapping mode of the rotor system can, for some designs, become low enough to require consideration in the assessment of handling characteristics (less than 2 Hz). This occurs for rotors with a large effective hinge offset and with heavy rotor blades.

INTRODUCTION

Continual improvement is sought in the inherent agility and stability of the helicopter to expand its operational capabilities while providing adequate safety margins. Recently, considerable emphasis has been placed on helicopter main rotor design features to enhance control moments and stability. Improvements in these areas are required, for instance, to permit single pilot commercial operation under instrument flight rules (IFR), and to provide the agility and maneuverability essential for nap-of-the-earth flight. The important design features include several that increase control moments by providing a direct hub moment in addition to that generated by thrust vector tilt. These features are the hingeless rotor (ref. 1) and the stiffened flapping hinge for the teetering rotor system (ref. 2). To improve the stability in forward flight, particularly with the hingeless rotor, consideration has been given to the use of mechanical means such as pitch-flap coupling (ref. 3). Safety of flight considerations, particularly for single-engine helicopters, leads to the high rotor inertia concept (ref. 4) to eliminate or reduce the dead man's height-velocity region.

Specific direct requirements may be achieved through the use of these main rotor design features. However, side effects, such as inter-axis coupling (ref. 5) and control response lag due to rotor dynamics, can adversely affect handling qualities. Insight on the potential impact of these design features on handling characteristics can be gained through a detailed examination of their effects on flapping dynamics. The analytical study reported herein provides this insight through consideration of the effects of large variation of flapping hinge offset, flapping hinge restraint, blade Lock number, and pitch-flap coupling on the flapping dynamics. Special emphasis was placed on determining the effects of these four design parameters on the tip-path plane dynamics and on the coupling of the longitudinal and lateral flapping due to control input and due to pitch and roll motion.

FLAPPING EQUATION OF MOTION

The flapping equation of motion was derived explicitly for a rotor system with the four parameters of interest, as shown in figure 1: the stiffness of the flapping hinge, K_β; the effective hinge offset, e; the blade Lock number, γ; and the pitch-flap coupling, K_1.

To develop analytical expressions that may provide a better insight into the parametric effects, many simplifications and assumptions similar to those used for the "classical" equations (ref. 6) were used. They are:

1. Rotor blade was rigid in bending and torsion, and the twist of the blade was linear.

2. Both the flapping angle and inflow angle were assumed to be small and the analysis utilized a simple strip theory.

3. The effects of the aircraft motion on the blade flapping were limited to those due to the angular acceleration $\dot{p}$ and $\dot{q}$, the angular rate p, q, and the normal acceleration.

4. The reversed flow region was ignored and the compressibility and stall effects disregarded.

5. The inflow was assumed to be uniform and no inflow dynamics were used.

6. The tip loss factor was assumed to be 1.

Because of these assumptions and simplifications, the results of the analysis were valid only for a limited range of flight conditions. Nevertheless, a previous study (ref. 7) has shown that this type of analysis is valid for stability and control investigations of the rotorcraft up to an advance ratio of approximately 0.3.

The development of the flapping equation of motion as described in appendix A was rather elementary and straightforward. The wind-hub coordinate

system, x_s, y_s, z_s, as depicted in figure 2, was employed as the basic frame of reference. In this coordinate system, x_s, y_s lie on the hub plane of the rotor, and the x_s-z_s plane contains the relative wind.

For nonteetering rotor systems, the flapping equation for a single blade was obtained by summing the moments due to aerodynamic forces acting on the blade, the centrifugal force, Coriolis, inertia, restraint forces, and the blade weight about the flapping hinge. The terms containing the hinge offset were retained up to the second power. The result as derived in appendix A is shown in equation (1).

$$\ddot{\beta}_i + \frac{\gamma\Omega}{2}\left[\left(\frac{1}{4} - \frac{2}{3}\varepsilon + \frac{\varepsilon^2}{2}\right) + \mu\left(\frac{1}{3} - \varepsilon + \varepsilon^2\right)\sin\psi_i\right]\dot{\beta}_i + \Omega^2\left\{p^2 + \frac{\gamma}{2}\left[\mu\left(\frac{1}{3} - \frac{\varepsilon}{2}\right)\cos\psi_i + \frac{\mu^2}{2}\left(\frac{1}{2} - \varepsilon + \frac{\varepsilon^2}{2}\right)\sin 2\psi_i\right] + \frac{\gamma K_1}{2}\left[\mu\left(\frac{2}{3} - \varepsilon\right)\sin\psi_i + \frac{\mu^2}{2}\left(\frac{1}{2} - \varepsilon + \frac{\varepsilon^2}{2}\right)\left(1 - \cos 2\psi_i\right)\right]\right\}\beta_i$$

$$= \Omega^2\left\{2\left(1 + \frac{eM_\beta}{I_\beta}\right)\left(-\frac{q_w}{\Omega}\sin\psi_i + \frac{p_w}{\Omega}\cos\psi_i\right) + \frac{\dot{p}_w}{\Omega^2}\sin\psi_i + \frac{\dot{q}_w}{\Omega^2}\cos\psi_i + \frac{M_\beta}{I_\beta\Omega^2}\left[(\dot{w} - uq + pv) - g\right] + \frac{\gamma}{2}\left[\left(\frac{1}{4} - \frac{\varepsilon}{3}\right) + \left(\frac{2}{3} - \varepsilon\right)\mu\sin\psi_i + \frac{\mu^2}{2}\left(\frac{1}{2} - \varepsilon + \frac{\varepsilon^2}{2}\right)\left(1 - \cos 2\psi_i\right)\right]\theta_0 - \frac{\gamma}{2}\left[\left(\frac{1}{4} - \frac{\varepsilon}{3}\right)\cos\psi_i + \mu\left(\frac{1}{3} - \frac{\varepsilon}{2}\right)\sin 2\psi_i + \frac{\mu^2}{4}\left(\frac{1}{2} - \varepsilon + \frac{\varepsilon^2}{2}\right)\left(\cos\psi_i - \cos 3\psi_i\right)\right]A_{1c} - \frac{\gamma}{2}\left[\left(\frac{1}{4} - \frac{\varepsilon}{3}\right)\sin\psi_i + \mu\left(\frac{1}{3} - \frac{\varepsilon}{2}\right)\left(1 - \cos 2\psi_i\right) + \frac{\mu^2}{4}\left(\frac{1}{2} - \varepsilon + \frac{\varepsilon^2}{2}\right)(3\sin\psi_i - \sin 3\psi_i)\right]B_{1c} + \frac{\gamma}{2}\left[\left(\frac{1}{5} - \frac{\varepsilon}{4}\right) + \mu\left(\frac{1}{2} - \frac{2}{3}\varepsilon\right)\sin\psi_i + \frac{\mu^2}{2}\left(\frac{1}{3} - \frac{\varepsilon}{2}\right)\left(1 - \cos 2\psi_i\right)\right]\theta_t + \frac{\gamma}{2}\left[\left(\frac{1}{3} - \frac{\varepsilon}{2}\right) + \mu\left(\frac{1}{2} - \varepsilon + \frac{\varepsilon^2}{2}\right)\sin\psi_i\right]\lambda\right\} + \frac{\gamma}{2}\left(\frac{1}{4} - \frac{\varepsilon}{3}\right)\left(\frac{p_w}{\Omega}\sin\psi_i + \frac{q_w}{\Omega}\cos\psi_i\right) + \frac{\gamma}{8}\mu\left(\frac{2}{3} - \varepsilon\right)\left[\frac{p_w}{\Omega}\left(1 - \cos 2\psi_i\right) + \frac{q_w}{\Omega}\sin 2\psi_i\right] \qquad (1)$$

where

$$P^2 = 1 + \frac{eM_\beta}{I_\beta} + \frac{K_\beta}{I_\beta \Omega^2} + \frac{\gamma K_1}{8}\left(1 - \frac{4}{3}\varepsilon\right)$$

$$i = 1, 2, 3, \ldots, N$$

$$p_w = p \cos \beta_w + q \sin \beta_w$$

$$q_w = -p \sin \beta_w + q \cos \beta_w$$

For a two-bladed teetering rotor, the flapping equation was derived from equation (1) using the following constraints:

$$\varepsilon = 0 \qquad \beta_2 = -\beta_1$$

$$\psi_2 = \psi_1 + \pi \qquad \dot{\beta}_2 = -\dot{\beta}_1 , \quad \ddot{\beta}_2 = -\ddot{\beta}_1$$

The result is shown in the following:

$$\ddot{\beta} + \frac{\Omega\gamma}{8}\dot{\beta} + \Omega^2\left[P^2 + \frac{\gamma\mu^2}{8}\sin 2\psi + \frac{\gamma K_1 \mu^2}{8}(1 - \cos 2\psi)\right]\beta$$

$$= \Omega^2\left\{\left(\frac{\gamma}{8}\frac{P_w}{\Omega} - 2\frac{q_w}{\Omega} + \frac{\dot{P}_w}{\Omega^2}\right)\sin\psi + \left(\frac{\gamma}{8}\frac{q_w}{\Omega} + 2\frac{P_w}{\Omega} + \frac{\dot{q}_w}{\Omega^2}\right)\cos\psi\right.$$

$$+ \left(\frac{\gamma\mu}{3}\sin\psi\right)\theta_0 - \frac{\gamma}{8}\left[\left(1 + \frac{\mu^2}{2}\right)\cos\psi - \frac{\mu^2}{2}\cos 3\psi\right]A_{1c} - \frac{\gamma}{8}\left[\left(1 + \frac{3}{2}\mu^2\right)\sin\psi\right.$$

$$\left.\left. - \frac{\mu^2}{2}\sin 3\psi\right]B_{1c} + \frac{\gamma\mu}{4}[\theta_t + \lambda]\sin\psi\right\} \tag{2}$$

where

$$P^2 = 1 + \frac{K_\beta}{I_\beta \Omega^2} + \frac{K_1 \gamma}{8}$$

To gain a better insight into the dynamics of the flapping motion, equation (1) will be transformed into a nonrotating coordinate system using the multibladed coordinate transformation (ref. 8), that is,

$$\beta_i = \beta_0 + \beta_d(-1)^i + \sum_{n=1}^{k} \beta_{nc} \cos n\psi_i + \beta_{ns} \sin n\psi_i$$

$$i = 1, 2, 3, \ldots, N \tag{3}$$

where

$$k = \frac{1}{2}(N - 1) \qquad N \text{ odd}$$

$$= \frac{1}{2}(N - 2) \qquad N \text{ even}$$

$$\beta_0 = \frac{1}{N}\sum_{i=1}^{N} \beta_i$$

$$\beta_d = \frac{1}{N}\sum_{i=1}^{N} \beta_i(-1)^i \qquad (\beta_d = 0, \text{ if } N \text{ odd})$$

$$\beta_{nc} = \frac{2}{N}\sum_{i=1}^{N} \beta_i \cos n\psi_i$$

$$\beta_{ns} = \frac{2}{N}\sum_{i=1}^{N} \beta_i \sin n\psi_i$$

$$\psi_i = \psi + \frac{2\pi}{N}(i - 1)$$

Let $\underline{\beta}_R$ and $\underline{\beta}$ be denoted, respectively, by

$$\underline{\beta}_R \triangleq (\beta_1, \beta_2, \ldots, \beta_N)^T$$

$$\underline{\beta} \triangleq (\beta_0, \beta_{1c}, \beta_{1s}, \beta_{2c}, \beta_{2s}, \ldots, \beta_{(1/2)(N-1)c}, \beta_{(1/2)(N-1)s})^T \qquad \text{for } N = \text{odd}$$

$$\triangleq (\beta_0, \beta_{1c}, \beta_{1s}, \ldots, \beta_{(1/2)(N-2)c}, \beta_{(1/2)(N-2)s}, \beta_d)^T \qquad \text{for } N = \text{even}$$

Then, as shown in appendix B, the flapping equation (1) in the rotating coordinate system may be transformed into the nonrotating coordinate system to yield:

$$\ddot{\underline{\beta}} + D\dot{\underline{\beta}} + K\underline{\beta} = \underline{f} \tag{4}$$

Tables 1 and 2 show the flapping equation in the nonrotating coordinate system for the three-bladed and four-bladed rotor systems, respectively. From these tables, the following observations may be made:

(a) In nonrotating coordinates, the flapping equations also contain periodic coefficients in forward flight. The basic frequency of the periodicity is directly related to the number of blades in the rotor; the basic frequency is 3 per rev for the three-bladed rotor and 2 per rev for the four-bladed rotor. The highest frequency in the periodic terms is N per rev for an N-bladed rotor. In general, it can be shown (as previously stated in ref. 9) that for 3, 5, 7, . . . bladed rotors, the basic frequency is 3, 5, 7, . . ., respectively; for 4, 6, 8, . . . bladed rotors, the corresponding basic frequency is 2, 3, 4, ...

(b) The amplitudes of the periodic terms in the damping matrix are functions of γ, ε, and μ; they are independent of K_β and K_1. At a given advance ratio, the lower the Lock number of the blade and the larger the hinge offset, the smaller the amplitudes of the periodic terms in the damping matrix.

(c) The maximum magnitude of the periodic coefficients in the stiffness matrix are functions of γ, ε, and K_1. Again the hinge restraint has no direct impact on the periodic terms. At a given advance ratio, a decrease in the blade Lock number will decrease the amplitude of the periodic terms in the stiffness matrix. However, the combined effect of ε and K_1 is more complicated. For $K_1 = 0$, an increase in the hinge offset will reduce the effect of the periodic terms.

(d) The parametric effect on the periodic terms in the forcing functions is similar to that on the damping terms for a given set of control positions, θ_0, A_{1c}, B_{1c}, and for the twist of the blade θ_t.

The above observations may provide a better insight in assessing the quality of approximation when the time varying flapping equations (expressed in the nonrotating coordinate system) in forward flight are simplified to time invariant system of equations by dropping the periodic terms. At $\mu = 0$, of course, there will be no periodic terms in these equations.

With the periodic terms dropped, the first three equations in table 2 for $N = 4$ collapse to those in table 1 for $N = 3$; the differential coning equation (the fourth equation) becomes uncoupled and with zero forcing function. The set of the first three equations is identical to the first-harmonic approximation also known as the "tip-path plane" equation as discussed in the next section.

TIP-PATH PLANE DYNAMICS

The mathematical procedure for approximating the flapping equation by performing the multiblade coordinate transformation and then dropping the periodic terms as discussed in the previous section is identical to the classical method of approximating the flapping by the first-harmonic terms with time varying coefficients, that is,

$$\beta(t) = a_0(t) - a_1(t)\cos\psi - b_1(t)\sin\psi \tag{5}$$

Equating, respectively, the constant term, and the terms with $\sin\psi$ and $\cos\psi$ in the equation (1) using (5), yields the tip-path plane dynamic equations:

$$\ddot{\underline{a}} + \tilde{D}\dot{\underline{a}} + \tilde{K}\underline{a} = \underline{\tilde{f}} \tag{6}$$

The damping matrix $\tilde{D}$, the stiffness matrix $\tilde{K}$, and the forcing function $\underline{\tilde{f}}$ are shown in table 3. This set of equations is identical to that in table 1, with periodic terms dropped. The identity is readily seen by noting that

$a_0 = \beta_0$, $a_1 = -\beta_{1c}$, and $b_1 = -\beta_{1s}$, and by performing a similarity transformation for the dynamic equations.

If the "tip-path plane" representation procedure described above is extended to approximate the flapping equation for the teetering rotor, equation (2) becomes

$$\begin{bmatrix} \ddot{a}_1 \\ \ddot{b}_1 \end{bmatrix} + \Omega \begin{bmatrix} \frac{\gamma}{8} & 2 \\ -2 & \frac{\gamma}{8} \end{bmatrix} \begin{bmatrix} \dot{a}_1 \\ \dot{b}_1 \end{bmatrix} + \Omega^2 \begin{bmatrix} p^2 - 1 + \frac{\gamma K_1 \mu^2}{16} & \frac{\gamma}{8}\left(1 + \frac{\mu^2}{2}\right) \\ -\frac{\gamma}{8}\left(1 - \frac{\mu^2}{2}\right) & p^2 - 1 + \frac{3}{16}\gamma K_1 \mu^2 \end{bmatrix} \begin{bmatrix} a_1 \\ b_1 \end{bmatrix}$$

$$= \Omega^2 \begin{bmatrix} 0 & 0 & \frac{\gamma}{8}\left(1 + \frac{\mu^2}{2}\right) & 0 \\ -\frac{\gamma\mu}{3} & -\frac{\gamma\mu}{4} & 0 & \frac{\gamma}{8}\left(1 + \frac{3}{2}\mu^2\right) \end{bmatrix} \begin{bmatrix} \theta_0 \\ \theta_t \\ A_{1c} \\ B_{1c} \end{bmatrix} + \Omega^2 \begin{bmatrix} 0 \\ -\frac{\gamma\mu}{4} \end{bmatrix} \lambda$$

$$+ \Omega \begin{bmatrix} -2 & -\frac{\gamma}{8} & 0 & -\frac{1}{\Omega} \\ -\frac{\gamma}{8} & 2 & -\frac{1}{\Omega} & 0 \end{bmatrix} \begin{bmatrix} p_w \\ q_w \\ \dot{p}_w \\ \dot{q}_w \end{bmatrix} \tag{7}$$

where

$$p^2 = 1 + \frac{K_\beta}{I_\beta \Omega^2} + \frac{\gamma K_1}{8}$$

and

$$\beta(t) = a_0 - a_1(t)\cos\psi - b_1(t)\sin\psi \tag{8}$$

Note that in equation (8), which approximates the flapping, the coning angle a_0 is a constant (a precone angle). The tip-path plane approximation for a two-bladed rotor is generally valid for only low frequency excitation; hence, the terms containing aircraft angular acceleration $\dot{p}$ and $\dot{q}$ in equation (7) may be omitted.

Equation (7) is identical to the lower 2×2 block shown in table 3 with ε set to zero. The quality of this approximation to the flapping equation of a teetering rotor system has not been fully evaluated. A preliminary numerical assessment showed that for $\mu > 0.4$,[1] the approximation in terms of stability characteristics could deteriorate rapidly, especially when $K_1 = K_\beta = 0$. A further evaluation is therefore needed to fully explore its limitations.

[1]Of course, at this condition, the validity of the model has already been violated, as described earlier in the report.

The dynamic characteristics of the tip-path plane as governed by the equations in table 3 will now be examined. There are three natural modes in the tip-path plane dynamics: coning, advancing, and regressing. Of these, the regressing flapping mode is most important concerning the effect of rotor dynamics on the handling characteristics of the rotorcraft. The regressing flapping mode is the lowest frequency mode of the three and it has a tendency to couple into the fuselage modes. The other two modes (the coning and the advancing) have higher undamped natural frequencies, respectively, on the order of rotating frequency and twice the rotating frequency of the rotor system; their impact on the rotorcraft handling characteristics is therefore considerably less significant.

To gain insight into the effects of the parametric variations in the general rotor system on the modal characteristics, hover conditions will be considered first. At hover, the coning equation is decoupled as evidenced in table 3. The coning mode has the undamped natural frequency ω_{nc} and the damping ratio ζ_c, respectively, as follows:

$$\left.\begin{aligned} \frac{\omega_{nc}}{\Omega} &= P \triangleq \left[1 + \frac{K_\beta}{I_\beta \Omega^2} + \frac{eM_\beta}{I_\beta} + \frac{\gamma K_1}{8}\left(1 - \frac{4}{3}\varepsilon\right)\right]^{1/2} \\ \zeta_c &= \zeta \triangleq \frac{\gamma}{16P}\left(1 - \frac{8}{3}\varepsilon + 2\varepsilon^2\right) \end{aligned}\right\} \tag{9}$$

The undamped natural frequency and the damping ratio for the advancing and regressing modes are, respectively, given by

$$\left.\begin{aligned} \frac{\omega_{nA}}{\Omega} &= \left(1 + P^2 + 2P\sqrt{1 - \zeta^2}\right)^{1/2} \\ \zeta_A &= \frac{\zeta}{\omega_{nA}/\Omega} \end{aligned}\right\} \tag{10a}$$

$$\left.\begin{aligned} \frac{\omega_{nR}}{\Omega} &= \left(1 + P^2 - 2P\sqrt{1 - \zeta^2}\right)^{1/2} \\ \zeta_R &= \frac{\zeta}{\omega_{nR}/\Omega} \end{aligned}\right\} \tag{10b}$$

Figures 3 through 5 show the effect of individual parametric variation in hinge offset, hinge restraint, and the pitch-flap feedback on the eigenvalues of the advancing and regressing modes. The effect on the blade Lock number is also shown in these figures which illustrate that γ is the most significant parameter in reducing the undamped natural frequency of the regressing flapping mode. If we concentrate on the region $\omega_{nR}/\Omega \leq 0.5$ (which corresponds to the region with undamped natural frequency of the regressing flapping mode of no more than 2.5 Hz for a 300 rpm main rotor system), the effect of a large hinge offset is also very significant in reducing ω_{nR} up to $\gamma = 12$. Thus, for a

small γ and a large ε, significant impact of the flapping dynamics on the handling characteristics of the rotorcraft can be expected.

In forward flight, the coning equation is no longer decoupled and the modal characteristics of the tip-path plane dynamics become much more complicated. Figures 6 through 9 show the effect of advance ratio on the eigenvalues of the three modes for four sets of parameter values, respectively:

$$K_\beta = \varepsilon = K_1 = 0$$

$$\varepsilon = 0.15 , \quad K_\beta = K_1 = 0$$

$$\frac{K_\beta}{I_\beta \Omega^2} = 0.225 , \quad \varepsilon = K_1 = 0$$

$$K_1 = 0.225 , \quad K_\beta = \varepsilon = 0$$

As indicated in these figures, the tip-path plane dynamic modes are relatively insensitive to the variation in the advance ratio μ (up to the validity of the math model, $\mu = 0.3$ to 0.4) for $\gamma < 8$. With a large hinge offset, the eigenvalues of the TPP modes are almost invariant over the entire range of Lock number considered.

As described earlier, the advancing mode of the TPP dynamics is on the order of 2 per rev (i.e., on the order of 10 Hz for a 300 rpm rotor system). Thus, the model will not be useful for real-time simulation if the computational cycle time is larger than $4\pi/\Omega$ (or on the order of 0.050 sec for a 300 rpm rotor system). If the budgeted cycle time cannot be reduced, some simplified models that will approximate the low frequency characteristics of the TPP dynamics may be desirable. A simple model that matches well with the equations in table 3 in the low frequency region may be obtained by simply setting $\ddot{\underline{a}} = 0$, as suggested in reference 9. The result is

$$\dot{\underline{a}} = - \tilde{D}^{-1} \tilde{K} \underline{a} + \tilde{D}^{-1} \tilde{\underline{f}} \tag{11}$$

Figures 10 through 12 show the comparison of characteristic roots of the reduced order model and the unreduced model at hover. For a forward flight at $\mu = 0.3$, their characteristic roots are shown in table 4. The fidelity in the transient response is shown in figures 13 and 14.

CONTROL PHASING AND FLAPPING RESPONSE DECOUPLING

It is evident from equation (6) and table 3 that the flapping frequency will generally be different from the rotational frequency of the rotor system. Therefore, the maximum flapping response to a cyclic-control input will no longer exhibit 90° lag in phase. Proper control phasing or control mixing will be required to achieve the desired flapping decoupling; a longitudinal control

input produces only a steady-state longitudinal flapping, and a lateral control input will produce only the lateral flapping response.

To relate the required control phasing (or control mixing) to the rotor system parameters, consider first the steady-state solution of TPP variables at hover. From equation (6), the steady-state responses of the TPP variables a_0, a_1, and b_1 to the control inputs and the fuselage angular velocity p_w and q_w may be obtained using

$$\underline{a}_{s.s.} = \tilde{K}^{-1}\tilde{\underline{f}} \tag{12}$$

At hover, equation (12) becomes

$$a_{0_{s.s.}} = \frac{1}{P^2}\left\{\frac{-gM_\beta}{I_\beta\Omega^2} + \frac{\gamma}{2}\left[\left(\frac{1}{4} - \frac{\varepsilon}{3}\right)\theta_0 + \left(\frac{1}{5} - \frac{\varepsilon}{4}\right)\theta_t + \left(\frac{1}{3} - \frac{\varepsilon}{2}\right)\lambda\right]\right\} \tag{13a}$$

$$a_{1_{s.s.}} = \frac{1}{\Delta}\left\{\gamma\left(\frac{1}{8} - \frac{\varepsilon}{6}\right)\left[(p^2 - 1)\left(A_{1c} - \frac{q_w}{\Omega}\right) - \gamma\left(\frac{1}{8} - \frac{\varepsilon}{3} + \frac{\varepsilon^2}{4}\right)\left(B_{1c} - \frac{p_w}{\Omega}\right)\right]\right.$$
$$\left. - 2\left(1 + \frac{eM_\beta}{I_\beta}\right)\left[(P^2 - 1)\frac{p_w}{\Omega} + \gamma\left(\frac{1}{8} - \frac{\varepsilon}{3} + \frac{\varepsilon^2}{4}\right)\frac{q_w}{\Omega}\right]\right\} \tag{13b}$$

$$b_{1_{s.s.}} = \frac{1}{\Delta}\left\{\gamma\left(\frac{1}{8} - \frac{\varepsilon}{6}\right)\left[\gamma\left(\frac{1}{8} - \frac{\varepsilon}{3} + \frac{\varepsilon^2}{4}\right)\left(A_{1c} - \frac{q_w}{\Omega}\right) + (p^2 - 1)\left(B_{1c} - \frac{p_w}{\Omega}\right)\right]\right.$$
$$\left. - 2\left(1 + \frac{eM_\beta}{I_\beta}\right)\left[\gamma\left(\frac{1}{8} - \frac{\varepsilon}{3} + \frac{\varepsilon^2}{4}\right)\frac{p_w}{\Omega} - (P^2 - 1)\frac{q_w}{\Omega}\right]\right\} \tag{13c}$$

where

$$\Delta = (P^2 - 1)^2 + \gamma^2\left(\frac{1}{8} - \frac{\varepsilon}{3} + \frac{\varepsilon^2}{4}\right)^2$$

$$P^2 = 1 + \frac{K_\beta}{I_\beta\Omega^2} + \frac{eM_\beta}{I_\beta} + \frac{\gamma K_1}{8}\left(1 - \frac{4}{3}\varepsilon\right)$$

In equations (13b) and (13c), the terms containing the fuselage angular accelerations, $\dot{p}$ and $\dot{q}$, have been dropped to be consistent with the steady-state solution of the TPP variables. From these equations, it is interesting to note that, for the special case $P^2 = 1$, $\varepsilon = 0$, the steady-state responses of the longitudinal and lateral flapping to the cyclic-control inputs reduce to the well known results:

$$a_{1_{s.s.}} = -B_{1c}$$

$$b_{1_{s.s.}} = A_{1c}$$

Feedforward Control Law

We will now develop the feedforward control law to achieve an appropriate control mixing for decoupling the steady-state flapping response to control displacements in the cockpit. To facilitate the flight-control system mechanization, the development will be based on the hub-body coordinate system. In this coordinate system, the cyclic pitch will be denoted by A_{1s} and B_{1s} and the tip-path plane tilt by a_{1s} and b_{1s}. They relate to those in the wind-hub system by the transformation:

$$A_{1c} = A_{1s} \cos \beta_w - B_{1s} \sin \beta_w$$

$$B_{1c} = A_{1s} \sin \beta_w + B_{1s} \cos \beta_w$$

$$a_1 = a_{1s} \cos \beta_w - b_{1s} \sin \beta_w$$

$$b_1 = a_{1s} \sin \beta_w + b_{1s} \cos \beta_w$$

Consider the hovering flight first. At hover, the longitudinal and lateral flapping depend on both A_{1c} and B_{1c}, but not on the collective pitch; the coning depends only on the collective pitch as evident from equations (13a), (13b), and (13c). Therefore, to decouple the steady-state flapping response, a control mixing of the following form will be satisfactory.

$$A_{1s} = \frac{\partial A_{1s}}{\partial \delta_A} \delta_A + \frac{\partial A_{1s}}{\partial \delta_L} \delta_L$$

$$B_{1s} = \frac{\partial B_{1s}}{\partial \delta_A} \delta_A + \frac{\partial B_{1s}}{\partial \delta_L} \delta_L$$

In the above equations, δ_A and δ_L are, respectively, the lateral and longitudinal control displacement at the cockpit. The control gearings

$$\frac{\partial A_{1s}}{\partial \delta_A}, \quad \frac{\partial A_{1s}}{\partial \delta_L}, \quad \frac{\partial B_{1s}}{\partial \delta_A}, \quad \frac{\partial B_{1s}}{\partial \delta_L}$$

for mixing the cyclic pitch may be chosen to satisfy a set of specified flapping response characteristics. Let the desired decoupled steady-state responses be

$$\frac{\partial a_{1s}}{\partial \delta_L} = k_1, \quad \frac{\partial b_{1s}}{\partial \delta_L} = 0$$

$$\frac{\partial b_{1s}}{\partial \delta_A} = k_2, \quad \frac{\partial a_{1s}}{\partial \delta_A} = 0$$

where the parameters k_1 and k_2 are the desired levels of control sensitivity.

From the previous static cyclic flapping equation, the control gearings may be readily found to be

$$\left.\begin{aligned}
\frac{\partial A_{1s}}{\partial \delta_A} &= \frac{1 - (8/3)\epsilon + 2\epsilon^2}{1 - (4/3)\epsilon}\, k_2 \\
\frac{\partial B_{1s}}{\partial \delta_B} &= \frac{8(P^2 - 1)}{\gamma[1 - (4/3)\epsilon]}\, k_2 \\
\frac{\partial A_{1s}}{\partial \delta_L} &= \frac{8(P^2 - 1)}{\gamma[1 - (4/3)\epsilon]}\, k_1 \\
\frac{\partial B_{1s}}{\partial \delta_L} &= \frac{-[1 - (8/3)\epsilon + 2\epsilon^2]}{1 - (4/3)\epsilon}\, k_1
\end{aligned}\right\} \tag{14}$$

with

$$P^2 - 1 = \frac{K_\beta}{I_\beta \Omega^2} + \frac{eM_\beta}{I_\beta} + \frac{\gamma K_1}{8}\left(1 - \frac{4}{3}\epsilon\right)$$

Alternately, if the control gearings $\partial A_{1s}/\partial \delta_A$ and $\partial B_{1s}/\partial \delta_L$ have been selected, decoupling the steady-state flapping may be achieved by appropriately phasing the cyclic-pitch control. The required control phasing (sometimes called control advance angle) in the sense of rotor rotation is given by $\phi = \tan^{-1}[(\partial B_{1s}/\partial \delta_A)/(\partial A_{1s}/\partial \delta_A)]$ or

$$\phi = \tan^{-1}\left[\frac{P^2 - 1}{\gamma[(1/8) - (\epsilon/3) + (\epsilon^2/4)]}\right] \tag{15}$$

Physically, the required control advance angle may be seen even more clearly by considering the flapping motion in the rotational coordinate. At hover, the flapping motion is governed by a second-order time invariant system with a natural frequency of $P\Omega$ and a damping ratio of $\gamma/P[(1/16) - (\epsilon/3) + (\epsilon^2/8)]$, as evident from equation (1). At the excitation frequency Ω, at which the cyclic pitch applies, the flapping response will have $(90° - \phi)$ lag in phase. For $P = 1$, when the flapping frequency is equal to the rotational frequency, then $\phi = 0$, as is well known.

In forward flight, the coning is coupled to the cyclic flapping. To achieve a perfect decoupling a control law which utilizes a mixing of the cyclic stick to the collective pitch as well as the cyclic pitch is required. The development of the control law is given in appendix C.

For a two-bladed teetering rotor system, a direct application of equation (14) to equation (7) results in the following feedforward control law:

$$K_{D_t} \triangleq \begin{bmatrix} \frac{\partial A_{1s}}{\partial \delta_A} & \frac{\partial A_{1s}}{\partial \delta_L} \\ \frac{\partial B_{1s}}{\partial \delta_A} & \frac{\partial B_{1s}}{\partial \delta_L} \end{bmatrix}$$

$$= \begin{bmatrix} k_2 & \frac{8}{\gamma}\left[\frac{P^2 - 1 + (\gamma K_1 \mu^2/16)}{1 + (\mu^2/2)}\right] k_1 \\ \frac{8}{\gamma}\left[\frac{P^2 - 1 + (3/16)\gamma K_1 \mu^2}{1 + (3/2)\mu^2}\right] k_2 & -\left[\frac{1 - (\mu^2/2)}{1 + (3/2)\mu^2}\right] k_1 \end{bmatrix} \tag{16}$$

It is interesting to note that equation (16) reduces to equation (14) at hover.

The decoupling control law equation (14) has been used previously in the nap-of-the-earth flight simulation (ref. 5) because of its simplicity in computer mechanization. The results have provided an approximation adequate for a speed range from hover up to an advance ratio of 0.25.

Decoupling Flapping Response Due to Aircraft Angular Rate

In the preceding discussion, attention has been focused on the decoupling of the flapping response to the control input. The other important aspect of decoupling the flapping response to the aircraft angular rate will now be discussed. Unlike fixed-wing aircraft, for which pitch-roll coupling is rare except in high angle-of-attack operations, rotorcraft often exhibit undesirable pitch-roll coupling due to aircraft angular motion. For example, in response to a roll rate to the right, the TPP tilts to the left to provide the desired roll damping of the aircraft; however, as is evident from equation (13b), the TPP plane can also accompany a tilt in the for-aft direction, which produces an undesirable pitching moment. Experiment (ref. 5) has indicated that this kind of pitch-roll coupling can adversely affect helicopter flying qualities, especially in demanding tasks such as in NOE or IFR operations. It is desirable, therefore, that the nature of the coupling in flapping due to aircraft angular rate be examined and a means of reducing the coupling be studied.

First, we shall examine the effect of the primary design parameters on the coupling. Consider the hover case. From equations (13b) and (13c), the steady-state response of the longitudinal and lateral flapping to the aircraft angular rate in pitch and roll is given by

$$\begin{bmatrix} a_1 \\ b_1 \end{bmatrix}_{s.s.} = \frac{1/\Omega}{(P^2 - 1)^2 + (\gamma^2/4)[(1/4) - (2/3)\varepsilon + (\varepsilon^2/2)]^2}$$

$$\times \begin{bmatrix} \frac{\gamma^2}{4}\left(\frac{1}{4} - \frac{2}{3}\varepsilon + \frac{\varepsilon^2}{2}\right)\left(\frac{1}{4} - \frac{\varepsilon}{3}\right) & -\gamma\left(1 + \frac{eM_\beta}{I_\beta}\right)\left(\frac{1}{4} - \frac{2}{3}\varepsilon + \frac{\varepsilon^2}{2}\right) \\ -2(P^2 - 1)\left(1 + \frac{eM_\beta}{I_\beta}\right) & -\frac{\gamma}{2}(P^2 - 1)\left(\frac{1}{4} - \frac{\varepsilon}{3}\right) \\ -\gamma\left(1 + \frac{eM_\beta}{I_\beta}\right)\left(\frac{1}{4} - \frac{2}{3}\varepsilon + \frac{\varepsilon^2}{2}\right) & -\frac{\gamma^2}{4}\left(\frac{1}{4} - \frac{2}{3}\varepsilon + \frac{\varepsilon^2}{2}\right)\left(\frac{1}{4} - \frac{\varepsilon}{3}\right) \\ -\frac{\gamma}{2}(P^2 - 1)\left(\frac{1}{4} - \frac{\varepsilon}{3}\right) & +2(P^2 - 1)\left(1 + \frac{eM_\beta}{I_\beta}\right) \end{bmatrix} \begin{bmatrix} p_w \\ \\ \\ q_w \end{bmatrix} \tag{17}$$

In particular, when $\varepsilon = 0$ and $P = 1$, equation (17) reduces to the following well known result:

$$\begin{pmatrix} a_1 \\ b_1 \end{pmatrix}_{s.s.} = \begin{pmatrix} \frac{1}{\Omega} & -\frac{16}{\gamma\Omega} \\ -\frac{16}{\gamma\Omega} & \frac{-1}{\Omega} \end{pmatrix} \begin{pmatrix} p_w \\ q_w \end{pmatrix} \tag{18}$$

It is clear from equation (17) that either a pitch rate or a roll rate input will produce steady-state responses in both longitudinal and lateral flapping unless the following condition is satisfied:

$$P^2 - 1 = \frac{(\gamma^2/4)[(1/4) - (\varepsilon/3)][(1/4) - (2/3)\varepsilon + (\varepsilon^2/2)]}{2[1 + (eM_\beta/I_\beta)]} \tag{19}$$

where

$$P^2 = 1 + \frac{K_\beta}{I_\beta\Omega^2} + \frac{eM_\beta}{I_\beta} + \frac{\gamma K_1}{8}\left(1 - \frac{4}{3}\varepsilon\right)$$

When the decoupling condition equation (19) is met, then

$$\frac{\partial a_{1_{s.s.}}}{\partial p_w} = 0$$

$$\frac{\partial b_{1_{s.s.}}}{\partial q_w} = 0$$

and

$$\frac{\partial a_{1_{s.s.}}}{\partial q_w} = \frac{\partial b_{1_{s.s.}}}{\partial p_w}$$

$$= \frac{-1/\Omega[(\gamma/4) + (\gamma/8)(P^2 - 1)]}{(P^2 - 1)^2 + (\gamma^2/4)[(1/4) - (2/3)\varepsilon + (\varepsilon^2/2)]^2} \tag{20}$$

The physical meaning of the decoupling condition is given in the following:

Consider the steady-state response of the longitudinal flapping a_1 due to aircraft roll rate p_w. From equation (17),

$$a_{1_{s.s.}} = \frac{p_w/\Omega}{(P^2 - 1)^2 + (\gamma^2/4)[(1/4) - (2/3)\varepsilon + (\varepsilon^2/2)]^2}\left[\frac{\gamma^2}{4}\left(\frac{1}{4} - \frac{2}{3}\varepsilon + \frac{\varepsilon^2}{2}\right)\left(\frac{1}{4} - \frac{\varepsilon}{3}\right) - 2(P^2 - 1)\left(1 + \frac{eM_\beta}{I_\beta}\right)\right] \tag{21}$$

Note that $b_{1_{s.s.}}$ due to q_w has the identical expression. From the derivation of the flapping equation, it can be seen that the first term in brackets in equation (21) is due to aerodynamic source while the second term is due to inertia. Thus, for $P = 1$ (the flapping frequency being 1 per rev), the inertia term vanishes, leaving only the aerodynamic contribution; in particular, for $\varepsilon = 0$ and $P = 1$, $a_{1_{s.s.}} = p_w/\Omega$, as shown earlier in equation (18). However, the flapping frequency may be changed appropriately by varying the hinge restraint, pitch-flap coupling, and hinge offset to achieve the level of inertia effect that offsets that due to aerodynamics. The condition for the inertia effect to cancel perfectly with the aerodynamic effect is essentially what equation (19) physically means.

It may be instructive to examine in some detail some special cases of the decoupling condition, equation (19), and the associated flapping responses, equation (20).

1. Rotor system with no flapping hinge offset— With $\varepsilon = 0$, the decoupling condition reduces to

$$P^2 - 1 = \frac{\gamma^2}{128} \tag{22a}$$

or

$$\frac{\gamma K_1}{8} + \frac{K_\beta}{I_\beta \Omega^2} = \frac{\gamma^2}{128} \tag{22b}$$

and the associated steady-state flapping becomes

$$\frac{\partial a_1}{\partial q_w}_{s.s.} = \frac{\partial b_1}{\partial p_w}_{s.s.}$$

$$= -\frac{16}{\gamma\Omega} \tag{23}$$

It is interesting to note that the condition for decoupling the flapping responses due to aircraft angular rates p and q for the center-hinged rotor cannot be met without using either the pitch-flap coupling or hinge restraint, or both, as is evident from equation (18). Furthermore, when the decoupling condition is met, the flapping responses are identical to those for $P = 1$, irrespective of the values for K_1 and K_β.

Figure 15 shows the pitch-flap coupling required to decouple the steady-state flapping response due to aircraft angular rate, p and q, for a center-hinged rotor system. The required pitch-flap coupling is shown as a function of the Lock number and the hinge restraint. As can be seen from this figure, the value of the pitch-flap coupling in the sense of reducing the pitch for positive flapping (upward) increases as γ increases and decreases somewhat as K_β increases.

2. Rotor system without flapping hinge restraint— With $K_\beta = 0$, equation (23) becomes

$$\frac{eM_\beta}{I_\beta} + \frac{\gamma K_1}{8}\left(1 - \frac{4}{3}\varepsilon\right) = \frac{(\gamma^2/4)[(1/4) - (\varepsilon/3)][(1/4) - (2/3)\varepsilon + (\varepsilon^2/2)]}{2[1 + (eM_\beta/I_\beta)]} \tag{24}$$

Consider that the rectangular blade has a uniform mass distribution. Then $eM_\beta/I_\beta = 1.5\,\varepsilon$. The pitch-flap coupling required to decouple the steady-state flapping response to the aircraft angular rate is obtained from equation (24) as follows:

$$K_1 = \frac{\gamma}{16}\frac{1 - (8/3)\varepsilon + 2\varepsilon^2}{1 + (3/2)\varepsilon} - \frac{12}{\gamma}\frac{\varepsilon}{1 - (4/3)\varepsilon} \tag{25}$$

Figure 16 shows the pitch-flap coupling required to decouple the steady-state flapping due to aircraft angular rate, p and q, for $K_\beta = 0$. The required pitch-flap coupling is shown as a function of the Lock number and the hinge offset. Note that for $\varepsilon = 0$, it is identical with the curve in figure 15 for $K_\beta/I_\beta\Omega^2 = 0$. However, as hinge offset increases, the required pitch-flap coupling differs substantially from that for hinge restraint with equivalent hinge offset (e.g., $K_\beta/I_\beta\Omega^2 = 0.225$ has an equivalent hinge offset of $\varepsilon = 0.15$, as far as flapping frequency is concerned).

Figure 17 depicts the amount of hinge offset required to decouple the flapping response for a set of pitch-flap couplings. Note that for $K_1 = 0$,

the amount of hinge offset varies almost linearly with Lock number from $\varepsilon = 0.019$ for $\gamma = 2$ to $\varepsilon = 0.145$ for $\gamma = 8$.

Aside from choosing a set of appropriate design parameters to decouple the steady-state flapping response due to aircraft angular rate, as discussed above, a feedback control law may also be used to achieve the same objective. Consider a control law of the form

$$\begin{pmatrix} A_{1c} \\ B_{1c} \end{pmatrix} = K_f \begin{pmatrix} p_w \\ q_w \end{pmatrix} \tag{26}$$

which feeds back aircraft angular rate, p and q, to both longitudinal and lateral cyclic. The feedback gain matrix K_f is to be chosen to achieve the desired decoupling characteristics:

$$\begin{pmatrix} a_1 \\ b_1 \end{pmatrix}_{s.s.} = - \begin{pmatrix} 0 & k_3 \\ k_3 & 0 \end{pmatrix} \begin{pmatrix} p_w \\ q_w \end{pmatrix} \tag{27}$$

In equation (27), the parameter k_3 is a desired sensitivity. Using equations (13b) and (13c), it can be shown that the decoupling control law that achieves the decoupling characteristics of equation (27) is given by

$$K_f = \frac{-1}{\gamma[(1/8) - (\varepsilon/6)]} \begin{bmatrix} -\frac{2}{\Omega}\left(1 + \frac{eM_\beta}{I_\beta}\right) + \gamma k_3\left(\frac{1}{8} - \frac{\varepsilon}{3} + \frac{\varepsilon^2}{4}\right) & -\frac{\gamma}{\Omega}\left(\frac{1}{8} - \frac{\varepsilon}{6}\right) + k_3(P^2 - 1) \\ -\frac{\gamma}{\Omega}\left(\frac{1}{8} - \frac{\varepsilon}{6}\right) + k_3(P^2 - 1) & \frac{2}{\Omega}\left(1 + \frac{eM_\beta}{I_\beta}\right) - \gamma k_3\left(\frac{1}{8} - \frac{\varepsilon}{3} + \frac{\varepsilon^2}{4}\right) \end{bmatrix} \tag{28}$$

Note that the sensitivity parameter k_3 in equation (27) is closely related to the contribution of the main rotor system to the vehicle's damping in pitch and roll. Therefore, equation (28) provides an insight into the relationship among the decoupling control gains needed, the vehicle's damping in pitch and roll, and the rotor system parameters.

CONCLUDING REMARKS

The flapping equation of motion for a main rotor system that consists of four primary design parameters — flapping hinge restraint, flapping hinge offset, blade Lock number, and pitch-flap coupling — has been developed in this paper. Both teetering and nonteetering cases were considered in the development and the equation was presented in both rotating and nonrotating coordinate systems.

Numerical examination of the tip-path plane dynamics indicated that the frequency of the regressing flapping mode was within the pilot's effective frequency range (less than 2 Hz) when the Lock number was small (around 6 or less), especially when the hinge offset was large ($\varepsilon > 0.07$). It was recommended, therefore, that the effects of flapping dynamics should be considered in assessing the flight dynamics and handling qualities of hingeless rotor helicopters or helicopters with heavy rotor blades.

Study of the steady-state flapping response due to aircraft angular rate in pitch and roll at hover showed that there exists a condition for achieving a perfect decoupling, that is, roll rate results only in lateral flapping and pitch rate only in longitudinal flapping. The condition should prove useful in selecting appropriate values of the four design parameters to minimize undesirable pitch-roll coupling of helicopter flight dynamics, especially in demanding tasks such as nap-of-the-earth flight. A control law that feeds back aircraft angular rate in pitch and roll to both longitudinal and lateral cyclic can also be used to decouple the steady-state flapping response. It provides an insight into the relationship among the decoupling control gains needed, the vehicle's damping in pitch and roll, and the rotor system parameters.

The cyclic control phasing or control mixing necessary for decoupling the steady-state response of the longitudinal and lateral flapping has been developed for hover and for forward flight. Because of its simplicity, the decoupling control law for hovering flight has been used previously in a ground simulation. It has provided an accuracy adequate for the entire low speed flight regime.

Ames Research Center
National Aeronautics and Space Administration
Moffett Field, Calif. 94035, May 11, 1979

APPENDIX A

DERIVATION OF FLAPPING EQUATION

Using the assumptions described in "Flapping Equation of Motion" (p. 2 of this report), the flapping equation was derived by summing the moments at the flapping hinge.

$$M_A + M_{CF} + M_I + M_{Cor.} + M_R + M_{BA} + M_{BL} + M_w = 0 \qquad (A1)$$

where

M_A moment due to aerodynamic force acting on the blade

M_{CF} moment due to the centrifugal force, $M_{CF} = -\Omega^2[I_\beta \cos \beta + eM_\beta]\sin \beta$

M_I moment due to blade inertia, $M_I = -I_\beta \ddot{\beta}$

$M_{Cor.}$ moment due to Coriolis acceleration, $M_{Cor.} = 2[I_\beta + eM_\beta](p\Omega \cos \psi' - q\Omega \sin \psi')$

M_R restraint moment, $M_R = -K_\beta \beta$

M_{BA} moment due to body angular acceleration, $M_{BA} = I_\beta(\dot{p} \sin \psi' + \dot{q} \cos \psi')$

M_{BL} moment due to body normal acceleration, $M_{BL} = M_\beta(\dot{w} - uq + pv)$

M_w weight moment of the blade about the flapping hinge

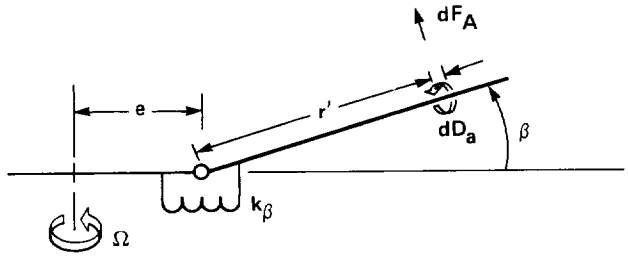

The moment due to the aerodynamic force acting on the blade, M_A, will now be derived in the following:

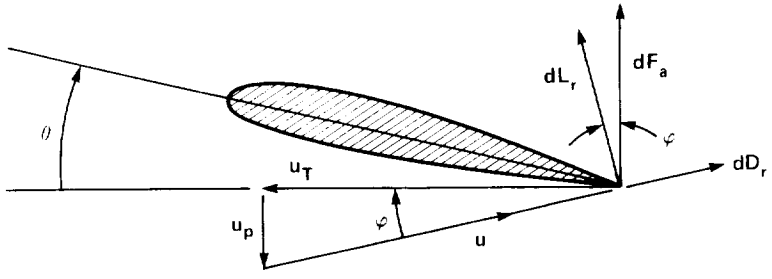

At an azimuth station ψ, M_A is given by

$$M_A = \int_0^{R-e} dF_a r'$$

where

$$dF_A = \frac{\rho}{2} (\Omega R)^2 ac[\bar{U}_T{}^2\theta + \bar{U}_T\bar{U}_P]dr'$$

and

$$\bar{U}_T \triangleq \frac{U_T}{\Omega R} = \varepsilon(1 - \cos\beta) + \mu \sin\psi + x\cos\beta$$

$$\bar{U}_p \triangleq \frac{U_p}{\Omega R} = \lambda\cos\beta - \mu\sin\beta\cos\psi - \bar{\beta}(x - \varepsilon) + x\left[\left(\frac{p}{\Omega}\cos\beta_w + \frac{q}{\Omega}\sin\beta_w\right)\sin\psi - \left(\frac{p}{\Omega}\sin\beta_w - \frac{q}{\Omega}\cos\beta_w\right)\cos\psi\right]$$

$$\mu \triangleq \frac{V\cos\alpha}{\Omega R}$$

$$\lambda \triangleq \frac{V\sin\alpha - v_i}{\Omega R}$$

$$x \triangleq \frac{e + r'}{R}, \qquad \varepsilon \triangleq \frac{e}{R}, \qquad \bar{\beta} \triangleq \frac{1}{\Omega}\dot{\beta}$$

$$\theta = \theta_0 - A_{1c}\cos\psi - \beta_{1c}\sin\psi + x\theta_t - K_1\beta$$

For small β,

$$\bar{U}_T = x + \mu\sin\psi$$

$$\bar{U}_p = \lambda - \mu\beta\cos\psi - \bar{\beta}(x - \varepsilon) + x\left[\left(\frac{p}{\Omega}\cos\beta_w + \frac{q}{\Omega}\sin\beta_w\right)\sin\psi - \left(\frac{p}{\Omega}\sin\beta_w - \frac{q}{\Omega}\cos\beta_w\right)\cos\psi\right]$$

and M_A may be found to be

$$\frac{M_A}{(\rho/2)ac(\Omega R)^2R^2} = \left[\frac{1}{4}(1-\varepsilon^4)+\frac{1}{3}(1-\varepsilon^3)(2\mu\sin\psi-\varepsilon)+\frac{1}{2}(1-\varepsilon^2)(\mu^2\sin^2\psi - 2\mu\varepsilon\sin\psi)-(1-\varepsilon)\mu^2\varepsilon\sin^2\psi\right](\theta_0 - A_{1c}\cos\psi - B_{1c}\sin\psi)$$

$$+\left[\frac{1}{5}(1-\varepsilon^5)+\frac{1}{4}(1-\varepsilon^4)(2\mu\sin\psi-\varepsilon) + \frac{1}{3}(1-\varepsilon^3)(\mu^2\sin^2\psi - 2\mu\varepsilon\sin\psi) - \frac{1}{2}(1-\varepsilon^2)\mu^2\varepsilon\sin^2\psi\right]\theta_t$$

$$+\left[\frac{1}{3}(1-\varepsilon^3)+\frac{1}{2}(1-\varepsilon^2)(\mu\sin\psi-\varepsilon)-(1-\varepsilon)\varepsilon\mu\sin\psi\right]\lambda$$

$$-\left\{\left[\frac{1}{4}(1-\varepsilon^4)+\frac{1}{3}(1-\varepsilon^3)(2\mu\sin\psi-\varepsilon) + \frac{1}{2}(1-\varepsilon^2)(\mu^2\sin^2\psi - 2\mu\varepsilon\sin\psi) - (1-\varepsilon)\mu^2\varepsilon\sin^2\psi\right]K_1\right.$$

$$\left.+\left[\frac{1}{3}(1-\varepsilon^3)+\frac{1}{2}(1-\varepsilon^2)(\mu\sin\psi-\varepsilon) - (1-\varepsilon)\mu\varepsilon\sin\psi\right]\mu\cos\psi\right\}\beta$$

$$-\left[\frac{1}{4}(1-\varepsilon^4)+\frac{1}{3}(1-\varepsilon^3)(\mu\sin\psi-2\varepsilon) - \frac{1}{2}(1-\varepsilon^2)(2\mu\varepsilon\sin\psi-\varepsilon^2)+(1-\varepsilon)\mu\varepsilon^2\sin\psi\right]\bar{\beta}$$

$$+\left[\frac{1}{4}(1-\varepsilon^4)+\frac{1}{3}(1-\varepsilon^3)(\mu\sin\psi-\varepsilon) - \frac{\mu\varepsilon}{2}(1-\varepsilon^2)\sin\psi\right]\left[\left(\frac{p}{\Omega}\cos\beta_w+\frac{q}{\Omega}\sin\beta_w\right)\sin\psi\right.$$

$$\left.-\left(\frac{p}{\Omega}\sin\beta_w-\frac{q}{\Omega}\cos\beta_w\right)\cos\psi\right] \qquad (A2)$$

Neglecting the terms containing ε^3, ε^4, . . ., the following result is obtained:

$$\frac{M_A}{(\rho/2)ac(\Omega R)^2R^2} = \left[\frac{1}{4} - \frac{\varepsilon}{3} + \mu \sin\psi\left(\frac{2}{3} - \varepsilon + \frac{1}{2}\mu \sin\psi - \varepsilon\mu \sin\psi + \frac{1}{2}\mu\varepsilon^2 \sin\psi\right)\right]$$

$$\times (\theta_0 - A_{1c}\cos\psi - B_{1c}\sin\psi) + \left[\frac{1}{5} - \frac{\varepsilon}{4} + \mu \sin\psi\left(\frac{1}{2} - \frac{2}{3}\varepsilon\right.\right.$$

$$\left.\left. + \frac{1}{3}\mu \sin\psi - \frac{1}{2}\mu\varepsilon \sin\psi\right)\right]\theta_t + \left[\frac{1}{3} - \frac{1}{2}\varepsilon + \mu \sin\psi\right.$$

$$\left.\times\left(\frac{1}{2} - \varepsilon + \frac{\varepsilon^2}{2}\right)\right]\lambda - \left\{\left[\frac{1}{4} - \frac{\varepsilon}{3} + \mu \sin\psi\left(\frac{2}{3} - \varepsilon + \frac{\mu}{2}\sin\psi\right.\right.\right.$$

$$\left.\left.\left. - \varepsilon\mu \sin\psi + \frac{\varepsilon^2}{2}\mu \sin\psi\right)\right]K_1 + \left[\frac{1}{3} - \frac{\varepsilon}{2} + \mu \sin\psi\left(\frac{1}{2} - \varepsilon\right.\right.\right.$$

$$\left.\left.\left. + \frac{\varepsilon^2}{2}\right)\right]\mu\cos\psi\right\}\beta - \left[\frac{1}{4} - \frac{2}{3}\varepsilon + \frac{\varepsilon^2}{2} + \mu \sin\psi\left(\frac{1}{3} - \varepsilon + \varepsilon^2\right)\right]\bar{\beta}$$

$$+ \left[\left(\frac{1}{4} - \frac{\varepsilon}{3}\right) + \mu \sin\psi\left(\frac{1}{3} - \frac{\varepsilon}{2}\right)\right]\left[\left(\frac{p}{\Omega}\cos\beta_w + \frac{q}{\Omega}\sin\beta_w\right)\sin\psi\right.$$

$$\left. - \left(\frac{p}{\Omega}\sin\beta_w - \frac{q}{\Omega}\cos\beta_w\right)\cos\psi\right] \qquad \text{(A3)}$$

The flapping equation is then obtained by substituting all the moments into equation (A1). The result becomes

$$\ddot{\beta} + \frac{\Omega\gamma}{2}\left[\frac{1}{4} - \frac{2}{3}\varepsilon + \frac{\varepsilon^2}{2} + \mu\left(\frac{1}{3} - \varepsilon + \varepsilon^2\right)\sin\psi\right]\dot{\beta} + \left(\left[\frac{K_\beta}{I_\beta} + \left(1 + \frac{eM_\beta}{I_\beta}\right)\Omega^2\right]\right.$$

$$+ \frac{\Omega^2\gamma}{2}\left\{\left[\frac{1}{4} - \frac{\varepsilon}{3} + \mu\left(\frac{2}{3} - \varepsilon + \frac{\mu}{2}\sin\psi - \varepsilon\mu \sin\psi + \frac{\varepsilon^2}{2}\mu \sin\psi\right)\sin\psi\right]K_1\right.$$

$$\left.\left. + \left[\frac{1}{3} - \frac{\varepsilon}{2} + \mu\left(\frac{1}{2} - \varepsilon + \frac{\varepsilon^2}{2}\right)\sin\psi\right]\mu\cos\psi\right\}\right)\beta$$

$$= 2\left(1 + \frac{eM_\beta}{I_\beta}\right)(p\Omega\cos\psi' - q\Omega\sin\psi') + (\dot{p}\sin\psi' + \dot{q}\cos\psi')$$

$$+ \frac{M_\beta}{I_\beta}(\dot{w} - uq + pv) - \frac{M_w}{I_\beta} + \frac{\Omega^2\gamma}{2}\left\{\left[\frac{1}{4} - \frac{\varepsilon}{3} + \mu \sin\psi\left(\frac{2}{3} - \varepsilon + \frac{1}{2}\mu \sin\psi\right.\right.\right.$$

$$\left.\left.\left. - \varepsilon\mu \sin\psi + \frac{1}{2}\mu\varepsilon^2 \sin\psi\right)\right](\theta_0 - A_{1c}\cos\psi - B_{1c}\sin\psi) + \left[\frac{1}{5} - \frac{\varepsilon}{4} + \mu\right.$$

$$\left.\times\left(\frac{1}{2} - \frac{2}{3}\varepsilon + \frac{1}{3}\mu \sin\psi - \frac{1}{2}\mu\varepsilon \sin\psi\right)\sin\psi\right]\theta_t + \left[\frac{1}{3} - \frac{1}{2}\varepsilon + \mu\right.$$

$$\left.\left.\times\left(\frac{1}{2} - \varepsilon + \frac{1}{2}\varepsilon^2\right)\sin\psi\right]\lambda\right\} + \frac{\gamma}{2}\left(\frac{1}{4} - \frac{\varepsilon}{3}\right)\left[(p\Omega\cos\beta_w + q\Omega\sin\beta_w)\sin\psi\right. \qquad \text{(A4)}$$

(Continued)

$$- (p\Omega \sin \beta_w - q\Omega \cos \beta_w)\cos \psi\Big] + \frac{\gamma}{8}\mu\left(\frac{2}{3} - \varepsilon\right)\Big[(p\Omega \cos \beta_w + q\Omega \sin \beta_w)$$

$$\times (1 - \cos 2\psi) - (p\Omega \sin \beta_w - q\Omega \cos \beta_w)\sin 2\psi\Big] \qquad \text{(A4)}$$

(Concluded)

where the Lock number γ is defined by

$$\gamma \triangleq \frac{\rho a c R^4}{I_\beta}$$

Equation (A4) may be rewritten in a nondimensional form by defining

$$\bar{\beta} \triangleq \frac{1}{\Omega}\dot{\beta} = \frac{d\beta}{d\psi}$$

$$\bar{\bar{\beta}} \triangleq \frac{1}{\Omega^2}\ddot{\beta} = \frac{d^2\beta}{d\psi^2}$$

The result becomes

$$\bar{\bar{\beta}} + \frac{\gamma}{2}\left[\frac{1}{4} - \frac{2}{3}\varepsilon + \frac{\varepsilon^2}{2} + \left(\frac{1}{3} - \varepsilon + \varepsilon^2\right)\mu \sin \psi\right]\bar{\beta} + \left\{\left(1 + \frac{eM_\beta}{I_\beta} + \frac{K_\beta}{I_\beta \Omega^2}\right)\right.$$

$$+ \frac{\gamma}{2}\left[\frac{1}{4} - \frac{\varepsilon}{3} + \left(\frac{2}{3} - \varepsilon + \frac{\mu}{2}\sin \psi - \varepsilon\mu \sin \psi + \frac{\varepsilon^2}{2}\mu \sin \psi\right)\mu \sin \psi\right]K_1$$

$$\left. + \left[\frac{1}{3} - \frac{\varepsilon}{2} + \left(\frac{1}{2} - \varepsilon + \frac{\varepsilon^2}{2}\right)\mu \sin \psi\right]\mu \cos \psi\right\}\beta$$

$$= 2\left(1 + \frac{eM_\beta}{I_\beta}\right)\left(\frac{p}{\Omega}\cos \psi' - \frac{q}{\Omega}\sin \psi'\right) + \left(\frac{\dot{p}}{\Omega^2}\sin \psi' + \frac{\dot{q}}{\Omega^2}\cos \psi'\right)$$

$$+ \frac{M_\beta}{\Omega^2 I_\beta}(\dot{w} - uq + pv) - \frac{M_w}{I_\beta \Omega^2} + \frac{\gamma}{2}\left\{\left[\frac{1}{4} - \frac{\varepsilon}{3} + \left(\frac{2}{3} - \varepsilon + \frac{1}{2}\mu \sin \psi - \varepsilon\mu \sin \psi\right.\right.\right.$$

$$\left.\left.\left. + \frac{1}{2}\mu\varepsilon^2 \sin \psi\right)\mu \sin \psi\right](\theta_0 - A_{1c}\cos \psi - B_{1c}\sin \psi) + \left[\frac{1}{5} - \frac{\varepsilon}{4}\right.$$

$$\left. + \left(\frac{1}{2} - \frac{2}{3}\varepsilon + \frac{1}{3}\mu \sin \psi - \frac{1}{2}\mu\varepsilon \sin \psi\right)\mu \sin \psi\right]\theta_t + \left[\frac{1}{3} - \frac{1}{2}\varepsilon\right.$$

$$\left. + \left(\frac{1}{2} - \varepsilon + \frac{1}{2}\varepsilon^2\right)\mu \sin \psi\right]\lambda\Big\} + \frac{\gamma}{2}\left(\frac{1}{4} - \frac{\varepsilon}{3}\right)\Big[\left(\frac{p}{\Omega}\cos \beta_w + \frac{q}{\Omega}\sin \beta_w\right)\sin \psi$$

$$- \left(\frac{p}{\Omega}\sin \beta_w - \frac{q}{\Omega}\cos \beta_w\right)\cos \psi\Big] + \frac{\gamma}{8}\mu\left(\frac{2}{3} - \varepsilon\right)\Big[\left(\frac{p}{\Omega}\cos \beta_w + \frac{q}{\Omega}\sin \beta_w\right)$$

$$\times (1 - \cos 2\psi) - \left(\frac{p}{\Omega}\sin \beta_w - \frac{q}{\Omega}\cos \beta_w\right)\sin 2\psi\Big] \qquad \text{(A5)}$$

APPENDIX B

TRANSFORMATION OF FLAPPING EQUATION FROM ROTATING TO NONROTATING COORDINATE SYSTEMS

In rotating coordinate systems, the flapping equation is given by equation (1) and is repeated here.

$$\ddot{\beta}_i + \frac{\gamma\Omega}{2}\left[\left(\frac{1}{4} - \frac{2}{3}\varepsilon + \frac{\varepsilon^2}{2}\right) + \mu\left(\frac{1}{3} - \varepsilon + \varepsilon^2\right)\sin\psi_i\right]\dot{\beta}_i + \Omega^2\left\{P^2 + \frac{\gamma}{2}\left[\mu\left(\frac{1}{3} - \frac{\varepsilon}{2}\right)\cos\psi_i + \frac{\mu^2}{2}\left(\frac{1}{2} - \varepsilon + \frac{\varepsilon^2}{2}\right)\sin 2\psi_i\right] + \frac{\gamma K_1}{2}\left[\mu\left(\frac{2}{3} - \varepsilon\right)\sin\psi_i + \frac{\mu^2}{2}\left(\frac{1}{2} - \varepsilon + \frac{\varepsilon^2}{2}\right)\left(1 - \cos 2\psi_i\right)\right]\right\}\beta_i$$

$$= \Omega^2\left\{2\left(1 + \frac{eM_\beta}{I_\beta}\right)\left(-\frac{q_w}{\Omega}\sin\psi_i + \frac{p_w}{\Omega}\cos\psi_i\right) + \frac{\dot{p}_w}{\Omega^2}\sin\psi_i + \frac{\dot{q}_w}{\Omega^2}\cos\psi_i + \frac{M_\beta}{I_\beta\Omega^2}\left[(\dot{w} - uq + pv) - g\right] + \frac{\gamma}{2}\left[\left(\frac{1}{4} - \frac{\varepsilon}{3}\right) + \left(\frac{2}{3} - \varepsilon\right)\mu\sin\psi_i + \frac{\mu^2}{2}\left(\frac{1}{2} - \varepsilon + \frac{\varepsilon^2}{2}\right)\left(1 - \cos 2\psi_i\right)\right]\theta_0 - \frac{\gamma}{2}\left[\left(\frac{1}{4} - \frac{\varepsilon}{3}\right)\cos\psi_i + \mu\left(\frac{1}{3} - \frac{\varepsilon}{2}\right)\sin 2\psi_i + \frac{\mu^2}{4}\left(\frac{1}{2} - \varepsilon + \frac{\varepsilon^2}{2}\right)\left(\cos\psi_i - \cos 3\psi_i\right)\right]A_{1c} - \frac{\gamma}{2}\left[\left(\frac{1}{4} - \frac{\varepsilon}{3}\right)\sin\psi_i + \mu\left(\frac{1}{3} - \frac{\varepsilon}{2}\right)\left(1 - \cos 2\psi_i\right) + \frac{\mu^2}{4}\left(\frac{1}{2} - \varepsilon + \frac{\varepsilon^2}{2}\right)(3\sin\psi_i - \sin 3\psi_i)\right]B_{1c} + \frac{\gamma}{2}\left[\left(\frac{1}{5} - \frac{\varepsilon}{4}\right) + \mu\left(\frac{1}{2} - \frac{2}{3}\varepsilon\right)\sin\psi_i + \frac{\mu^2}{2}\left(\frac{1}{3} - \frac{\varepsilon}{2}\right)(1 - \cos 2\psi_i)\right]\theta_t + \frac{\gamma}{2}\left[\left(\frac{1}{3} - \frac{\varepsilon}{2}\right) + \mu\left(\frac{1}{2} - \varepsilon + \frac{\varepsilon^2}{2}\right)\sin\psi_i\right]\lambda\right\} + \frac{\gamma}{2}\left(\frac{1}{4} - \frac{\varepsilon}{3}\right)\left(\frac{p_w}{\Omega}\sin\psi_i + \frac{q_w}{\Omega}\cos\psi_i\right) + \frac{\gamma}{8}\mu\left(\frac{2}{3} - \varepsilon\right)\left[\frac{p_w}{\Omega}(1 - \cos 2\psi_i) + \frac{q_w}{\Omega}\sin 2\psi_i\right] \tag{B1}$$

where

$$P^2 = 1 + \frac{eM_\beta}{I_\beta} + \frac{K_\beta}{I_\beta \Omega^2} + \frac{\gamma K_1}{8}\left(1 - \frac{4}{3}\epsilon\right)$$

$$i = 1, 2, 3, \ldots, N$$

$$p_w = p \cos \beta_w + q \sin \beta_w$$

$$q_w = -p \sin \beta_w + q \cos \beta_w$$

To gain a better insight into the dynamics of the flapping motion equation (1) will be transformed into a nonrotating coordinate system using the multibladed coordinate transformation (ref. 9), that is,

$$\beta_i = \beta_0 + \beta_d(-1)^i + \sum_{n=1}^{k} \beta_{nc} \cos n\psi_i + \beta_{ns} \sin n\psi_i \qquad (B2)$$

$$i = 1, 2, 3, \ldots, N$$

where

$$k = \frac{1}{2}(N - 1) \qquad N \text{ odd}$$

$$= \frac{1}{2}(N - 2) \qquad N \text{ even}$$

$$\beta_0 = \frac{1}{N}\sum_{i=1}^{N} \beta_i$$

$$\beta_d = \frac{1}{N}\sum_{i=1}^{N} \beta_i(-1)^i \qquad (\beta_d = 0, \text{ if } N \text{ odd})$$

$$\beta_{nc} = \frac{2}{N}\sum_{i=1}^{N} \beta_i \cos n\psi_i$$

$$\beta_{ns} = \frac{2}{N}\sum_{i=1}^{N} \beta_i \sin n\psi_i$$

$$\psi_i = \psi + \frac{2\pi}{N}(i - 1)$$

Let $\underline{\beta}_R$ and $\underline{\beta}$ be denoted, respectively, by

$$\underline{\beta}_R \triangleq (\beta_1, \beta_2, \ldots, \beta_N)^T$$

$$\underline{\beta} \triangleq (\beta_0, \beta_{1c}, \beta_{1s}, \beta_{2c}, \beta_{2s}, \ldots, \beta_{(1/2)(N-1)c}, \beta_{(1/2)(N-1)s})^T \qquad \text{for } N = \text{odd}$$

$$\triangleq (\beta_0, \beta_{1c}, \beta_{1s}, \ldots, \beta_{(1/2)(N-1)c}, \beta_{(1/2)(N-1)s}, \beta_d)^T \qquad \text{for } N = \text{even}$$

Then the transformation equation (B2) may be rewritten by

$$\underline{\beta}_R = T\underline{\beta} \tag{B3}$$

where, for N = odd

$$T = \begin{bmatrix} 1 & \cos\psi_1 & \sin\psi_1 & \cdots & \cos\frac{1}{2}(N-1)\psi_1 & \sin\frac{1}{2}(N-1)\psi_1 \\ 1 & \cos\psi_2 & \sin\psi_2 & & \cos\frac{1}{2}(N-1)\psi_2 & \sin\frac{1}{2}(N-1)\psi_2 \\ \vdots & \vdots & \vdots & & \vdots & \vdots \\ 1 & \cos\psi_i & \sin\psi_i & & \cos\frac{1}{2}(N-1)\psi_i & \sin\frac{1}{2}(N-1)\psi_i \\ \vdots & \vdots & \vdots & & \vdots & \vdots \\ 1 & \cos\psi_N & \sin\psi_N & & \cos\frac{1}{2}(N-1)\psi_N & \sin\frac{1}{2}(N-1)\psi_N \end{bmatrix}$$

and, for N = even

$$T = \begin{bmatrix} 1 & \cos\psi_1 & \sin\psi_1 & \cdots & \cos\frac{1}{2}(N-2)\psi_1 & \sin\frac{1}{2}(N-2)\psi_1 & (-1)^1 \\ 1 & \cos\psi_2 & \sin\psi_2 & & \cos\frac{1}{2}(N-2)\psi_2 & \sin\frac{1}{2}(N-2)\psi_2 & (-1)^2 \\ \vdots & \vdots & \vdots & & \vdots & \vdots & \vdots \\ 1 & \cos\psi_i & \sin\psi_i & & \cos\frac{1}{2}(N-2)\psi_i & \sin\frac{1}{2}(N-2)\psi_i & (-1)^i \\ \vdots & \vdots & \vdots & & \vdots & \vdots & \vdots \\ 1 & \cos\psi_{N-1} & \sin\psi_{N-1} & & \cos\frac{1}{2}(N-2)\psi_{N-1} & \sin\frac{1}{2}(N-2)\psi_{N-1} & (-1)^{N-1} \\ 1 & \cos\psi_N & \sin\psi_N & & \cos\frac{1}{2}(N-2)\psi_N & \sin\frac{1}{2}(N-2)\psi_N & (-1)^N \end{bmatrix}$$

$$\psi_i = \psi + \frac{2\pi}{N}(i-1), \qquad i = 1,2,3,\ldots,N$$

The flapping equation (A1) may now be rewritten in a matrix-vector format as follows:

$$\ddot{\underline{\beta}}_R + A(\psi)\dot{\underline{\beta}}_R + B(\psi)\underline{\beta}_R = \underline{f}_R \tag{B4}$$

where

$$A(\psi) = \begin{bmatrix} A_{11} & & & & \\ & \ddots & & 0 & \\ & & A_{ii} & & \\ & 0 & & \ddots & \\ & & & & A_{NN} \end{bmatrix}$$

$$B(\psi) = \begin{bmatrix} B_{11} & & & & \\ & \ddots & & 0 & \\ & & B_{ii} & & \\ & 0 & & \ddots & \\ & & & & B_{NN} \end{bmatrix}$$

$$\underline{f}_R \triangleq (f_1, f_2, \ldots, f_i, \ldots, f_N)^T$$

and

$$A_{ii} \triangleq \frac{\gamma\Omega}{2}\left[\left(\frac{1}{4} - \frac{2}{3}\varepsilon + \frac{\varepsilon^2}{2}\right) + \mu\left(\frac{1}{3} - \varepsilon + \varepsilon^2\right)\sin\psi_i\right]$$

$$B_{ii} \triangleq \Omega^2\left\{P^2 + \frac{\gamma}{2}\left[\mu\left(\frac{1}{3} - \frac{\varepsilon}{2}\right)\cos\psi_i + \frac{\mu^2}{2}\left(\frac{1}{2} - \varepsilon + \frac{\varepsilon^2}{2}\right)\sin 2\psi_i\right] + \frac{\gamma K_1}{2}\left[\mu\left(\frac{2}{3} - \varepsilon\right)\sin\psi_i + \frac{\mu^2}{2}\left(\frac{1}{2} - \varepsilon + \frac{\varepsilon^2}{2}\right)(1 - \cos 2\psi_i)\right]\right\}$$

$f_i \triangleq$ right-hand side of equation (B-1). (B4)

With respect to the nonrotating coordinate system $\underline{\beta}$, the flapping equation (B4) may be represented by (B5) using the transformation (B3).

$$\ddot{\underline{\beta}} + D\dot{\underline{\beta}} + K\underline{\beta} = \underline{f} \tag{B5}$$

where

$$\underline{f} = T^{-1}\underline{f}_R$$

$$D = T^{-1}(2\dot{T} + AT)$$

$$K = T^{-1}(\ddot{T} + A\dot{T} + BT)$$

To expedite the calculation of the inverse of T, a proper scaling of the variables $\underline{\beta}$ may be made so that

$$\underline{\beta} = T_S\underline{\beta}_I \tag{B6}$$

where

$$T_S = \begin{cases} \begin{bmatrix} \frac{1}{\sqrt{N}} & & & 0 \\ & \sqrt{\frac{2}{N}} & & \\ & & \ddots & \\ 0 & & & \sqrt{\frac{2}{N}} \end{bmatrix} & \text{for N odd} \\ \begin{bmatrix} \frac{1}{\sqrt{N}} & \sqrt{\frac{2}{N}} & & 0 \\ & & \ddots & \\ & & & \sqrt{\frac{2}{N}} \\ 0 & & & \frac{1}{\sqrt{N}} \end{bmatrix} & \text{for N even} \end{cases}$$

The resultant transformation $T_I = TT_S$ is orthogonal. Since $T^{-1} = T_S I_I^{-1} = T_S{}^2T'$, the desired simplification in computing T^{-1} is achieved.

Tables 1 and 2 show the results for N = 3 and N = 4, respectively. For a special case in which $K_1 = \varepsilon = 0$ and $\dot{p} = \dot{q} = p = q = 0$, the equations in these tables reduce to those previously obtained in reference 8.

APPENDIX C

FEEDFORWARD CONTROL LAW FOR DECOUPLING FLAPPING RESPONSE IN FORWARD FLIGHT

From table 3, it is evident that in forward flight the coning is coupled to the cyclic flapping. To achieve a perfect decoupling, a complete control mixing will be required

Consider a feedforward control law of the form

$$\begin{bmatrix} \theta_0 \\ A_{1s} \\ B_{1s} \end{bmatrix} = K_D \begin{bmatrix} \delta_c \\ \delta_A \\ \delta_L \end{bmatrix} \tag{C1}$$

where

$$K_D \triangleq \begin{bmatrix} \frac{\partial \theta_0}{\partial \delta_c} & \frac{\partial \theta_0}{\partial \delta_A} & \frac{\partial \theta_0}{\partial \delta_L} \\ \frac{\partial A_{1s}}{\partial \delta_c} & \frac{\partial A_{1s}}{\partial \delta_A} & \frac{\partial A_{1s}}{\partial \delta_L} \\ \frac{\partial B_{1s}}{\partial \delta_c} & \frac{\partial B_{1s}}{\partial \delta_A} & \frac{\partial A_{1s}}{\partial \delta_L} \end{bmatrix}$$

is the "control mixing" matrix. The control law is to be selected so as to achieve a desired decoupling in steady-state response having the sensitivities

$$k_0 \triangleq \frac{\partial a_0}{\partial \delta_c}, \quad k_1 \triangleq \frac{\partial a_{1s}}{\partial \delta_A}, \quad \text{and} \quad k_2 \triangleq \frac{\partial b_{1s}}{\partial \delta_L}$$

as follows:

$$\begin{bmatrix} a_0 \\ a_{1s} \\ b_{1s} \end{bmatrix}_{s.s.} = \begin{bmatrix} k_0 & 0 & 0 \\ 0 & 0 & k_1 \\ 0 & k_2 & 0 \end{bmatrix} \begin{bmatrix} \delta_c \\ \delta_A \\ \delta_L \end{bmatrix} \tag{C2}$$

Denote

$$\underline{a} \triangleq (a_0, a_{1s}, b_{1s})^T , \qquad \underline{u} \triangleq (\theta_0, A_{1s}, B_{1s})^T$$

$$\underline{u}_P \triangleq (\delta_c, \delta_A, \delta_L)^T$$

$$S \triangleq \begin{bmatrix} k_0 & 0 & 0 \\ 0 & 0 & k_1 \\ 0 & k_2 & 0 \end{bmatrix}$$

Let the control effective matrix E be

$$E = \Omega^2 \begin{bmatrix} \alpha_1 & 0 & \alpha_2 \\ 0 & \alpha_3 & 0 \\ \alpha_4 & 0 & \alpha_5 \end{bmatrix}$$

where

$$\alpha_1 = \frac{\gamma}{2}\left[\left(\frac{1}{4} - \frac{\varepsilon}{3}\right) + \frac{\mu^2}{2}\left(\frac{1}{2} - \varepsilon + \frac{\varepsilon^2}{2}\right)\right] + \Lambda_1$$

$$\alpha_2 = -\frac{\gamma}{2}\mu\left(\frac{1}{3} - \frac{\varepsilon}{2}\right)$$

$$\alpha_3 = \frac{\gamma}{2}\left[\left(\frac{1}{4} - \frac{\varepsilon}{3}\right) + \frac{\mu^2}{4}\left(\frac{1}{2} - \varepsilon + \frac{\varepsilon^2}{2}\right)\right]$$

$$\alpha_4 = -\frac{\gamma}{2}\mu\left(\frac{2}{3} - \varepsilon\right) + \Lambda_2$$

$$\alpha_5 = \frac{\gamma}{2}\left[\left(\frac{1}{4} - \frac{\varepsilon}{3}\right) + \frac{3\mu^2}{4}\left(\frac{1}{2} - \varepsilon + \frac{\varepsilon^2}{2}\right)\right]$$

and Λ_1 and Λ_2 account for the effect of inflow due to collective input, that is,

$$\Lambda_1 = \frac{\gamma}{2}\left(\frac{1}{3} - \frac{\varepsilon}{2}\right)\frac{\partial\lambda}{\partial\theta_0} , \text{ and } \Lambda_2 = -\frac{\gamma\mu}{2}\left(\frac{1}{2} - \varepsilon + \frac{\varepsilon^2}{2}\right)\frac{\partial\lambda}{\partial\theta_0}$$

The steady-state response of the coning and cyclic flapping to control input is given by

$$\underline{a}_{s.s.} = \tilde{K}^{-1}\tilde{\underline{f}}$$

$$= \tilde{K}^{-1}E\underline{u}$$

$$= \tilde{K}^{-1}EK_D\underline{u}_P$$

Imposing the desired decoupling characteristics as described in equation (C2), that is, $\underline{a}_{s.s.} = S\underline{u}_p$, the control law may be found to be

$$K_D = E^{-1}\tilde{K}S$$

It is readily verifiable that

$$E^{-1} = \frac{1}{\Omega^2(\alpha_1\alpha_5 - \alpha_2\alpha_4)} \begin{bmatrix} \alpha_5 & 0 & -\alpha_2 \\ 0 & \dfrac{\alpha_1\alpha_5 - \alpha_2\alpha_4}{\alpha_3} & 0 \\ -\alpha_4 & 0 & \alpha_1 \end{bmatrix} \tag{C3}$$

and the desired decoupling control law is obtained as described in equation (C4).

$$K_D = \frac{1}{\alpha_1\alpha_5 - \alpha_2\alpha_4}$$

$$\times \begin{bmatrix} \left\{\left[P^2 + \frac{\gamma K_1\mu^2}{4}\left(\frac{1}{2} - \varepsilon + \frac{\varepsilon^2}{2}\right)\right]\alpha_5 + \left[\frac{\gamma K_1\mu}{2}\left(\frac{2}{3} - \varepsilon\right)\right]\alpha_2\right\} k_0 & -\left\{\frac{\gamma K_1\mu}{4}\left(\frac{2}{3} - \varepsilon\right)\alpha_5 + \left[P^2 - 1 + \frac{3}{8}\gamma K_1\mu^2\left(\frac{1}{2} - \varepsilon + \frac{\varepsilon^2}{2}\right)\right]\alpha_2\right\} k_2 & -\left\{\left[\frac{\gamma\mu}{4}\left(\frac{\varepsilon}{2} - \varepsilon^2\right)\right]\alpha_5 + \left[-\frac{\gamma}{2} \times \left(\frac{1}{4} - \frac{2}{3}\varepsilon + \frac{\varepsilon^2}{2}\right) + \frac{\gamma\mu^2}{8} \times \left(\frac{1}{2} - \varepsilon + \frac{\varepsilon^2}{2}\right)\right]\alpha_2\right\} k_1 \\ -\left[\frac{\gamma\mu}{2}\left(\frac{1}{3} - \frac{\varepsilon}{2}\right)\frac{1}{\alpha_3}\left(\alpha_1\alpha_5 - \alpha_2\alpha_4\right)\right] k_0 & \left\{\left[\frac{\gamma}{2}\left(\frac{1}{4} - \frac{2}{3}\varepsilon + \frac{\varepsilon^2}{2}\right) + \frac{\gamma\mu^2}{8}\left(\frac{1}{2} - \varepsilon + \frac{\varepsilon^2}{2}\right)\right] \times \frac{1}{\alpha_3}\left(\alpha_1\alpha_5 - \alpha_2\alpha_4\right)\right\} k_2 & \left\{\left[P^2 - 1 + \frac{\gamma K_1\mu^2}{8}\left(\frac{1}{2} - \varepsilon + \frac{\varepsilon^2}{2}\right)\right] \times \frac{1}{\alpha_3}\left(\alpha_1\alpha_5 - \alpha_2\alpha_4\right)\right\} k_1 \\ -\left\{\left[P^2 + \frac{\gamma K_1\mu^2}{4}\left(\frac{1}{2} - \varepsilon + \frac{\varepsilon^2}{2}\right)\right]\alpha_4 + \frac{\gamma K_1\mu}{2}\left(\frac{2}{3} - \varepsilon\right)\alpha_1\right\} k_0 & \left\{\frac{\gamma K_1\mu}{4}\left(\frac{2}{3} - \varepsilon\right)\alpha_4 + \left[P^2 - 1 + \frac{3}{8}\gamma K_1\mu^2\left(\frac{1}{2} - \varepsilon + \frac{\varepsilon^2}{2}\right)\right]\alpha_1\right\} k_2 & \left\{\frac{\gamma\mu}{4}\left(\frac{\varepsilon}{2} - \varepsilon^2\right)\alpha_4 + \left[-\frac{\gamma}{2}\left(\frac{1}{4} - \frac{2}{3}\varepsilon + \frac{\varepsilon^2}{2}\right) + \frac{\gamma\mu^2}{8}\left(\frac{1}{2} - \varepsilon + \frac{\varepsilon^2}{2}\right)\right]\alpha_1\right\} k_1 \end{bmatrix}$$

(C4)

REFERENCES

1. Blake, B. B.; and Alansky, I. B.: Stability and Control of the YUH-61A. Paper presented at the 31st AHS National Forum, May 13-15, 1975.

2. Seibel, C. M.; and Kulik, C. M.: The Bell YAH-63 Advanced Attach Helicopter Configuration, Design Considerations, and Development Status. Paper presented at the 31st AHS National Forum, May 13-15, 1975.

3. Wood, T. L.: High Energy Rotor System. Paper presented at the 32nd Annual National Forum, May 10-12, 1976.

4. Hohenemser, K. H.: Hingeless Rotorcraft Flight Dynamics. AGARD-AG-197, Sept. 1974.

5. Chen, R. T. N.; and Talbot, P. D.: An Exploratory Investigation of the Effects of Large Variations in Rotor System Dynamics Design Parameters on Helicopter Handling Characteristics in Nap-of-the-Earth Flight. Paper presented at the 33rd AHS National Forum, May 9-11, 1977.

6. Gessow, A.; and Myers, G. C., Jr.: Aerodynamics of the Helicopter. Frederick Ungar Publishing Co., New York, 1952.

7. Seckel, E.; and Curtiss, H. C., Jr.: Aerodynamic Characteristics of Helicopter Rotors. Department of Aerospace and Mechanical Engineering Report No. 659, Princeton University, Princeton, New Jersey, Dec. 1963.

8. Hohenemser, K. H.; and Yin, S. K.: Some Applications of the Method of Multiblade Coordinates. J. American Helicopter Soc., vol. 17, no. 3, 1972, pp. 3-12.

9. Hohenemser, K. H.; and Yin, S. K.: On the Use of First Order Rotor Dynamics in Multiblade Coordinates. Paper presented at 30th Annual National Forum, May 7-9, 1974.

TABLE 1.- FLAPPING EQUATION IN NONROTATING COORDINATE SYSTEM, N = 3

$$\ddot{\underline{\beta}} + D_3\dot{\underline{\beta}} + K_3\underline{\beta} = \underline{f}_3 \; ; \qquad \underline{\beta} \triangleq (\beta_0, \beta_{1c}, \beta_{1s})^T$$

$$D_3 = \Omega \begin{bmatrix} \gamma\left(\frac{1}{8} - \frac{\varepsilon}{3} + \frac{\varepsilon^2}{4}\right) & 0 & \frac{1}{4}\gamma\mu\left(\frac{1}{3} - \varepsilon + \varepsilon^2\right) \\ 0 & \gamma\left(\frac{1}{8} - \frac{\varepsilon}{3} + \frac{\varepsilon^2}{4}\right) + \frac{\gamma\mu}{4}\left(\frac{1}{3} - \varepsilon + \varepsilon^2\right)\sin 3\psi & 2 - \frac{\gamma\mu}{4}\left(\frac{1}{3} - \varepsilon + \varepsilon^2\right)\cos 3\psi \\ \frac{1}{2}\gamma\mu\left(\frac{1}{3} - \varepsilon + \varepsilon^2\right) & -2 - \frac{\gamma\mu}{4}\left(\frac{1}{3} - \varepsilon + \varepsilon^2\right)\cos 3\psi & \gamma\left(\frac{1}{8} - \frac{\varepsilon}{3} + \frac{\varepsilon^2}{4}\right) - \frac{\gamma\mu}{4}\left(\frac{1}{3} - \varepsilon + \varepsilon^2\right)\sin 3\psi \end{bmatrix}$$

$$K_3 = \Omega^2 \begin{bmatrix} P^2 + \frac{\gamma K_1\mu^2}{4}\left(\frac{1}{2} - \varepsilon + \frac{\varepsilon^2}{2}\right) & \frac{\gamma\mu}{4}\left(\frac{\varepsilon}{2} - \varepsilon^2\right) + \frac{\gamma\mu^2}{8} \times \left(\frac{1}{2} - \varepsilon + \frac{\varepsilon^2}{2}\right)\sin 3\psi - \frac{\gamma\mu^2 K_1}{8} \times \left(\frac{1}{2} - \varepsilon + \frac{\varepsilon^2}{2}\right)\cos 3\psi & \frac{\gamma\mu K_1}{4}\left(\frac{2}{3} - \varepsilon\right) - \frac{\gamma\mu^2}{8} \times \left(\frac{1}{2} - \varepsilon + \frac{\varepsilon^2}{2}\right)\cos 3\psi - \frac{\gamma\mu^2 K_1}{8}\left(\frac{1}{2} - \varepsilon + \frac{\varepsilon^2}{2}\right)\sin 3\psi \\ \frac{1}{2}\gamma\mu\left(\frac{1}{3} - \frac{\varepsilon}{2}\right) + \frac{\gamma\mu^2}{4} \times \left(\frac{1}{2} - \varepsilon + \frac{\varepsilon^2}{2}\right)\sin 3\psi - \frac{\gamma\mu^2 K_1}{4}\left(\frac{1}{2} - \varepsilon + \frac{\varepsilon^2}{2}\right)\cos 3\psi & P^2 - 1 + \frac{\gamma\mu^2 K_1}{8}\left(\frac{1}{2} - \varepsilon + \frac{\varepsilon^2}{2}\right) + \frac{\gamma\mu}{4}\left(\frac{2}{3} - \frac{3\varepsilon}{2} + \varepsilon^2\right)\cos 3\psi + \frac{\gamma\mu K_1}{4}\left(\frac{2}{3} - \varepsilon\right)\sin 3\psi & \frac{\gamma}{2}\left[\left(\frac{1}{4} - \frac{2}{3}\varepsilon + \frac{\varepsilon^2}{2}\right) + \frac{\mu^2}{4}\left(\frac{1}{2} - \varepsilon + \frac{\varepsilon^2}{2}\right)\right] + \frac{\gamma\mu}{4}\left(\frac{2}{3} - \frac{3\varepsilon}{2} + \varepsilon^2\right)\sin 3\psi - \frac{\gamma\mu K_1}{4}\left(\frac{2}{3} - \varepsilon\right)\cos 3\psi \\ \frac{\gamma\mu K_1}{2}\left(\frac{2}{3} - \varepsilon\right) - \frac{\gamma\mu^2}{4} \times \left(\frac{1}{2} - \varepsilon + \frac{\varepsilon^2}{2}\right)\cos 3\psi - \frac{\gamma\mu^2 K_1}{4}\left(\frac{1}{2} - \varepsilon + \frac{\varepsilon^2}{2}\right)\sin 3\psi & -\frac{\gamma}{2}\left[\left(\frac{1}{4} - \frac{2}{3}\varepsilon + \frac{\varepsilon^2}{2}\right) - \frac{\mu^2}{4}\left(\frac{1}{2} - \varepsilon + \frac{\varepsilon^2}{2}\right)\right] + \frac{\gamma\mu}{4}\left(\frac{2}{3} - \frac{3}{2}\varepsilon + \varepsilon^2\right) \times \sin 3\psi - \frac{\gamma\mu K_1}{4}\left(\frac{2}{3} - \varepsilon\right)\cos 3\psi & P^2 - 1 + \frac{3}{8}\gamma\mu^2 K_1\left(\frac{1}{2} - \varepsilon + \frac{\varepsilon^2}{2}\right) - \frac{\gamma\mu}{4}\left(\frac{2}{3} - \frac{3}{2}\varepsilon + \varepsilon^2\right)\cos 3\psi - \frac{\gamma\mu K_1}{4}\left(\frac{2}{3} - \varepsilon\right)\sin 3\psi \end{bmatrix}$$

$$P^2 = 1 + \frac{eM_\beta}{I_\beta} + \frac{K_\beta}{I_\beta\Omega^2} + \frac{\gamma K_1}{8}\left(1 - \frac{4}{3}\varepsilon\right)$$

TABLE 1.- Concluded.

$$
\underline{f}_3 = \Omega^2
\begin{bmatrix}
\frac{\gamma}{8}\left[\left(1 - \frac{4\varepsilon}{3}\right) + 2\mu^2\left(\frac{1}{2} - \varepsilon + \frac{\varepsilon^2}{2}\right)\right] & \frac{\gamma}{8}\left[\left(\frac{4}{5} - \varepsilon\right) + 2\mu^2 \times \left(\frac{1}{3} - \frac{\varepsilon}{2}\right)\right] & \frac{\gamma\mu^2}{8}\left(\frac{1}{2} - \varepsilon + \frac{\varepsilon^2}{2}\right)\cos 3\psi & -\frac{\gamma\mu}{8}\left[2\left(\frac{2}{3} - \varepsilon\right) - \mu \times \left(\frac{1}{2} - \varepsilon + \frac{\varepsilon^2}{2}\right)\sin 3\psi\right] \\
-\frac{\gamma\mu^2}{4}\left(\frac{1}{2} - \varepsilon + \frac{\varepsilon^2}{2}\right)\cos 3\psi & -\frac{\gamma\mu^2}{4}\left(\frac{1}{3} - \frac{\varepsilon}{2}\right)\cos 3\psi & -\frac{\gamma}{2}\left[\left(\frac{1}{4} - \frac{\varepsilon}{3}\right) + \frac{\mu^2}{4}\left(\frac{1}{2} - \varepsilon + \frac{\varepsilon^2}{2}\right) + \frac{1}{2}\left(\frac{2}{3} - \varepsilon\right) \times \mu \sin 3\psi\right] & -\frac{\mu}{4}\left(\frac{2}{3} - \varepsilon\right)\cos 3\psi \\
\frac{\gamma\mu}{2}\left[\left(\frac{2}{3} - \varepsilon\right) - \frac{\mu}{2} \times \left(\frac{1}{2} - \varepsilon + \frac{\varepsilon^2}{2}\right)\sin 3\psi\right] & \frac{\gamma\mu}{2}\left[\left(\frac{1}{2} - \frac{2\varepsilon}{3}\right) - \frac{\mu}{2} \times \left(\frac{1}{3} - \frac{\varepsilon}{2}\right)\sin 3\psi\right] & \frac{\gamma\mu}{4}\left(\frac{2}{3} - \varepsilon\right)\cos 3\psi & -\frac{\gamma}{4}\left[2\left(\frac{1}{4} - \frac{\varepsilon}{3}\right) + \frac{3\mu^2}{2} \times \left(\frac{1}{2} - \varepsilon + \frac{\varepsilon^2}{2}\right) - \mu\left(\frac{2}{3} - \varepsilon\right)\sin 3\psi\right]
\end{bmatrix}
\begin{bmatrix} \theta_0 \\ \theta_t \\ A_{1c} \\ B_{1c} \end{bmatrix}
$$

$$
+ \Omega^2
\begin{bmatrix}
\frac{\gamma\mu}{8\Omega}\left(\frac{2}{3} - \varepsilon\right) & 0 & 0 & 0 \\
\frac{2}{\Omega}\left[\left(1 + \frac{eM_\beta}{I_\beta}\right) - \frac{\gamma\mu}{16}\left(\frac{2}{3} - \varepsilon\right)\cos 3\psi\right] & \frac{\gamma}{2\Omega}\left(\frac{1}{4} - \frac{\varepsilon}{3}\right) + \frac{\mu}{4} \times \left(\frac{2}{3} - \varepsilon\right)\sin 3\psi & 0 & \frac{1}{\Omega^2} \\
\frac{\gamma}{2\Omega}\left[\left(\frac{1}{4} - \frac{\varepsilon}{3}\right) - \frac{\mu}{4}\left(\frac{2}{3} - \varepsilon\right)\sin 3\psi\right] & -\frac{2}{\Omega}\left[\left(1 - \frac{eM_\beta}{I_\beta}\right) + \frac{\gamma\mu}{16} \times \left(\frac{2}{3} - \varepsilon\right)\cos 3\psi\right] & \frac{1}{\Omega^2} & 0
\end{bmatrix}
\begin{bmatrix} p_w \\ q_w \\ \dot{p}_w \\ \dot{q}_w \end{bmatrix}
$$

$$
+ \Omega^2
\begin{bmatrix} \frac{\gamma}{2}\left(\frac{1}{3} - \frac{\varepsilon}{2}\right) \\ 0 \\ \frac{\gamma\mu}{2}\left(\frac{1}{2} - \varepsilon + \frac{\varepsilon^2}{2}\right) \end{bmatrix} \lambda
+
\begin{bmatrix} \frac{M_\beta}{I_\beta}\left[(\dot{w} - uq + pv) - g\right] \\ 0 \\ 0 \end{bmatrix}
$$

TABLE 2.- FLAPPING EQUATION IN NONROTATING COORDINATE SYSTEM, N = 4

$$\ddot{\underline{\beta}} + D_4\dot{\underline{\beta}} + K_4\underline{\beta} = \underline{f}_4;\ \underline{\beta} \triangleq (\beta_0, \beta_{1c}, \beta_{1s}, \beta_d)^T$$

$D_4 = \Omega$

$$\begin{bmatrix} \gamma\left(\frac{1}{8} - \frac{\varepsilon}{3} + \frac{\varepsilon^2}{4}\right) & 0 & \frac{\gamma\mu}{4}\left(\frac{1}{3} - \varepsilon + \varepsilon^2\right) & 0 \\ 0 & \gamma\left(\frac{1}{8} - \frac{\varepsilon}{3} + \frac{\varepsilon^2}{4}\right) & 2 & -\frac{\gamma\mu}{2}\left(\frac{1}{3} - \varepsilon + \varepsilon^2\right)\sin 2\psi \\ \frac{\gamma\mu}{2}\left(\frac{1}{3} - \varepsilon + \varepsilon^2\right) & -2 & \gamma\left(\frac{1}{8} - \frac{\varepsilon}{3} + \frac{\varepsilon^2}{4}\right) & \frac{\gamma\mu}{2}\left(\frac{1}{3} - \varepsilon + \varepsilon^2\right)\cos 2\psi \\ 0 & -\frac{\gamma\mu}{4}\left(\frac{1}{3} - \varepsilon + \varepsilon^2\right)\sin 2\psi & \frac{\gamma\mu}{4}\left(\frac{1}{3} - \varepsilon + \varepsilon^2\right)\cos 2\psi & \gamma\left(\frac{1}{8} - \frac{\varepsilon}{3} + \frac{\varepsilon^2}{4}\right) \end{bmatrix}$$

$K_4 = \Omega^2$

$$\begin{bmatrix} p^2 + \frac{\gamma K_1\mu^2}{4}\left(\frac{1}{2} - \varepsilon + \frac{\varepsilon^2}{2}\right) & \frac{\gamma\mu}{4}\left(\frac{\varepsilon}{2} - \varepsilon^2\right) & \frac{\gamma K_1\mu}{4}\left(\frac{2}{3} - \varepsilon\right) & \frac{\gamma\mu^2}{4}\left(\frac{1}{2} - \varepsilon + \frac{\varepsilon^2}{2}\right) \times (K_1\cos 2\psi - \sin 2\psi) \\ \frac{\gamma\mu}{2}\left(\frac{1}{3} - \frac{\varepsilon}{2}\right) & p^2 - 1 + \frac{K_1\gamma\mu^2}{8} \times \left(\frac{1}{2} - \varepsilon + \frac{\varepsilon^2}{2}\right) + \frac{\gamma\mu^2}{8}\left(\frac{1}{2} - \varepsilon + \frac{\varepsilon^2}{2}\right) \times (\sin 4\psi - K_1\cos 4\psi) & \gamma\left(\frac{1}{8} - \frac{\varepsilon}{3} + \frac{\varepsilon^2}{4}\right) + \frac{\gamma\mu^2}{8} \times \left(\frac{1}{2} - \varepsilon + \frac{\varepsilon^2}{2}\right) - \frac{\gamma\mu^2}{8} \times \left(\frac{1}{2} - \varepsilon + \frac{\varepsilon^2}{2}\right) \times (K_1\sin 4\psi + \cos 4\psi) & -\frac{\gamma\mu}{2}\left(\frac{1}{3} - \frac{\varepsilon}{2}\right) \times (2K_1\sin 2\psi + \cos 2\psi) \\ \frac{\gamma K_1\mu}{2}\left(\frac{2}{3} - \varepsilon\right) & -\gamma\left(\frac{1}{8} - \frac{\varepsilon}{3} + \frac{\varepsilon^2}{4}\right) + \frac{\gamma\mu^2}{8} \times \left(\frac{1}{2} - \varepsilon + \frac{\varepsilon^2}{2}\right) - \frac{\gamma\mu^2}{8}\left(\frac{1}{2} - \varepsilon + \frac{\varepsilon^2}{2}\right) \times (\cos 4\psi + K_1\sin 4\psi) & p^2 - 1 + \frac{3\gamma\mu^2 K_1}{8}\left(\frac{1}{2} - \varepsilon + \frac{\varepsilon^2}{2}\right) + \frac{\gamma\mu^2}{8} \times \left(\frac{1}{2} - \varepsilon + \frac{\varepsilon^2}{2}\right) \times (K_1\cos 4\psi - \sin 4\psi) & \frac{\gamma\mu}{2}\left(\frac{1}{3} - \frac{\varepsilon}{2}\right) \times (2K_1\cos 2\psi - \sin 2\psi) \\ \frac{\gamma\mu^2}{4}\left(\frac{1}{2} - \varepsilon + \frac{\varepsilon^2}{2}\right) \times (K_1\cos 2\psi - \sin 2\psi) & -\frac{\gamma K_1\mu}{4}\left(\frac{2}{3} - \varepsilon\right)\sin 2\psi - \frac{\gamma\mu}{4}\left(\frac{2}{3} - \frac{3\varepsilon}{2} + \varepsilon^2\right) \times \cos 2\psi & \frac{\gamma K_1\mu}{4}\left(\frac{2}{3} - \varepsilon\right)\cos 2\psi - \frac{\gamma\mu}{4}\left(\frac{2}{3} - \frac{3\varepsilon}{2} + \varepsilon^2\right)\sin 2\psi & p^2 + \frac{\gamma K_1}{4}\mu^2\left(\frac{1}{2} - \varepsilon + \frac{\varepsilon^2}{2}\right) \end{bmatrix}$$

TABLE 2.- Concluded.

$$
\underline{f}_{1_c} = \Omega^2 \begin{bmatrix}
\frac{\gamma}{8}\left[\left(1 - \frac{4}{3}\epsilon\right) + 2\mu^2 \times \left(\frac{1}{2} - \epsilon + \frac{\epsilon^2}{2}\right)\right] & \frac{\gamma}{8}\left[\left(\frac{4}{5} - \epsilon\right) + 2\mu^2 \times \left(\frac{1}{3} - \frac{\epsilon}{2}\right)\right] & 0 & -\frac{\gamma}{4}\mu\left(\frac{2}{3} - \epsilon\right) \\
0 & 0 & -\frac{\gamma}{2}\left[\left(\frac{1}{4} - \frac{\epsilon}{3}\right) + \frac{\mu^2}{4} \times \left(\frac{1}{2} - \epsilon + \frac{\epsilon^2}{2}\right) \times (1 - \cos 4\psi)\right] & \frac{\gamma\mu^2}{8}\left(\frac{1}{2} - \epsilon + \frac{\epsilon^2}{2}\right)\sin 4\psi \\
\frac{\gamma}{2}\mu\left(\frac{2}{3} - \epsilon\right) & \frac{\gamma\mu}{2}\left(\frac{1}{2} - \frac{2}{3}\epsilon\right) & \frac{\gamma\mu^2}{8}\left(\frac{1}{2} - \epsilon + \frac{\epsilon^2}{2}\right)\sin 4\psi & -\frac{\gamma}{4}\left[2\left(\frac{1}{4} - \frac{\epsilon}{3}\right) + \frac{\mu^2}{2} \times \left(\frac{1}{2} - \epsilon + \frac{\epsilon^2}{2}\right) \times (3 + \cos 4\psi)\right] \\
\frac{\gamma\mu^2}{4}\left(\frac{1}{2} - \epsilon + \frac{\epsilon^2}{2}\right)\cos 2\psi & \frac{\gamma\mu^2}{4}\left(\frac{1}{3} - \frac{\epsilon}{2}\right)\cos 2\psi & \frac{\gamma\mu}{4}\left(\frac{2}{3} - \epsilon\right)\sin 2\psi & -\frac{\gamma\mu}{4}\left(\frac{2}{3} - \epsilon\right)\cos 2\psi
\end{bmatrix}
\begin{bmatrix} \theta_0 \\ \theta_t \\ A_{1c} \\ B_{1c} \end{bmatrix}
$$

$$
+ \Omega \begin{bmatrix}
-\frac{\gamma\mu}{8\Omega}\left(\frac{2}{3} - \epsilon\right) & 0 & 0 & 0 \\
\frac{2}{\Omega}\left(1 + \frac{eM_\beta}{I_\beta}\right) & \frac{\gamma}{2\Omega}\left(\frac{1}{4} - \frac{\epsilon}{3}\right) & 0 & \frac{1}{\Omega^2} \\
\frac{\gamma}{2\Omega}\left(\frac{1}{4} - \frac{\epsilon}{3}\right) & -\frac{2}{\Omega}\left(1 + \frac{eM_\beta}{I_\beta}\right) & \frac{1}{\Omega^2} & 0 \\
0 & 0 & 0 & 0
\end{bmatrix}
\begin{bmatrix} p_w \\ q_w \\ \dot{p}_w \\ \dot{q}_w \end{bmatrix}
$$

$$
+ \Omega^2 \begin{bmatrix} \frac{\gamma}{2}\left(\frac{1}{3} - \frac{\epsilon}{2}\right) \\ 0 \\ \frac{\gamma\mu}{2}\left(\frac{1}{2} - \epsilon + \frac{\epsilon^2}{2}\right) \\ 0 \end{bmatrix} \lambda + \begin{bmatrix} \frac{M_\beta}{I_\beta}\left[(\dot{w} - uq + pv) - g\right] \\ 0 \\ 0 \\ 0 \end{bmatrix}
$$

$$
p^2 \triangleq 1 + \frac{eM_\beta}{I_\beta} + \frac{K_\beta}{I_\beta \Omega^2} + \frac{\gamma K_1}{8}\left(1 - \frac{4}{3}\epsilon\right)
$$

TABLE 3.- TIP-PATH PLANE EQUATION

$$\ddot{\underline{a}} + \tilde{D}\dot{\underline{a}} + \tilde{K}\underline{a} = \tilde{f}$$

$$\tilde{D} = \Omega \begin{bmatrix} \frac{\gamma}{2}\left(\frac{1}{4} - \frac{2}{3}\varepsilon + \frac{\varepsilon^2}{2}\right) & 0 & -\frac{\gamma\mu}{4}\left(\frac{1}{3} - \varepsilon + \varepsilon^2\right) \\ 0 & \frac{\gamma}{2}\left(\frac{1}{4} - \frac{2}{3}\varepsilon + \frac{\varepsilon^2}{2}\right) & 2 \\ -\frac{\gamma\mu}{2}\left(\frac{1}{3} - \varepsilon + \varepsilon^2\right) & -2 & \frac{\gamma}{2}\left(\frac{1}{4} - \frac{2}{3}\varepsilon + \frac{\varepsilon^2}{2}\right) \end{bmatrix}$$

$$\tilde{K} = \Omega^2 \begin{bmatrix} p^2 + \frac{\gamma K_1 \mu^2}{4}\left(\frac{1}{2} - \varepsilon + \frac{\varepsilon^2}{2}\right) & -\frac{\gamma\mu}{4}\left(\frac{\varepsilon}{2} - \varepsilon^2\right) & -\frac{\gamma K_1 \mu}{4}\left(\frac{2}{3} - \varepsilon\right) \\ -\frac{\gamma\mu}{2}\left(\frac{1}{3} - \frac{\varepsilon}{2}\right) & p^2 - 1 + \frac{\gamma K_1 \mu^2}{8}\left(\frac{1}{2} - \varepsilon + \frac{\varepsilon^2}{2}\right) & \frac{\gamma}{2}\left(\frac{1}{4} - \frac{2}{3}\varepsilon + \frac{\varepsilon^2}{2}\right) + \frac{\gamma\mu^2}{8} \times \left(\frac{1}{2} - \varepsilon + \frac{\varepsilon^2}{2}\right) \\ -\frac{\gamma K_1 \mu}{2}\left(\frac{2}{3} - \varepsilon\right) & -\frac{\gamma}{2}\left(\frac{1}{4} - \frac{2}{3}\varepsilon + \frac{\varepsilon^2}{2}\right) + \frac{\gamma\mu^2}{8} \times \left(\frac{1}{2} - \varepsilon + \frac{\varepsilon^2}{2}\right) & p^2 - 1 + \frac{3}{8}\gamma K_1 \mu^2\left(\frac{1}{2} - \varepsilon + \frac{\varepsilon^2}{2}\right) \end{bmatrix}$$

$$\tilde{f} = \Omega^2 \begin{bmatrix} \frac{\gamma}{2}\left[\left(\frac{1}{4} - \frac{\varepsilon}{3}\right) + \frac{\mu^2}{2} \times \left(\frac{1}{2} - \varepsilon + \frac{\varepsilon^2}{2}\right)\right] & \frac{\gamma}{2}\left[\left(\frac{1}{5} - \frac{\varepsilon}{4}\right) + \frac{\mu^2}{2} \times \left(\frac{1}{3} - \frac{\varepsilon}{2}\right)\right] & 0 & -\frac{\gamma\mu}{2}\left(\frac{1}{3} - \frac{\varepsilon}{2}\right) \\ 0 & 0 & \frac{\gamma}{2}\left[\left(\frac{1}{4} - \frac{\varepsilon}{3}\right) + \frac{\mu^2}{4} \times \left(\frac{1}{2} - \varepsilon + \frac{\varepsilon^2}{2}\right)\right] & 0 \\ -\frac{\gamma}{2}\mu\left(\frac{2}{3} - \varepsilon\right) & -\frac{\gamma\mu}{2}\left(\frac{1}{2} - \frac{2\varepsilon}{3}\right) & 0 & \frac{\gamma}{2}\left[\left(\frac{1}{4} - \frac{\varepsilon}{3}\right) + \frac{3\mu^2}{4} \times \left(\frac{1}{2} - \varepsilon + \frac{\varepsilon^2}{2}\right)\right] \end{bmatrix} \begin{bmatrix} \theta_0 \\ \theta_t \\ A_{1c} \\ B_{1c} \end{bmatrix}$$

$$+ \Omega^2 \begin{bmatrix} \frac{\gamma\mu}{8\Omega}\left(\frac{2}{3} - \varepsilon\right) & 0 & 0 & 0 \\ -\frac{2}{\Omega}\left(1 + \frac{eM_\beta}{I_\beta}\right) & -\frac{\gamma}{2\Omega}\left(\frac{1}{4} - \frac{\varepsilon}{3}\right) & 0 & -\frac{1}{\Omega^2} \\ -\frac{\gamma}{2\Omega}\left(\frac{1}{4} - \frac{\varepsilon}{3}\right) & \frac{2}{\Omega}\left(1 + \frac{eM_\beta}{I_\beta}\right) & -\frac{1}{\Omega^2} & 0 \end{bmatrix} \begin{bmatrix} p_w \\ q_w \\ \dot{p}_w \\ \dot{q}_w \end{bmatrix}$$

$$+ \Omega^2 \begin{bmatrix} \frac{\gamma}{2}\left(\frac{1}{3} - \frac{\varepsilon}{2}\right) \\ 0 \\ -\frac{\gamma\mu}{2}\left(\frac{1}{2} - \varepsilon + \frac{\varepsilon^2}{2}\right) \end{bmatrix} \lambda + \begin{bmatrix} \frac{M_\beta}{I_\beta}\left[(\dot{w} - uq + pv) - g\right] \\ 0 \\ 0 \end{bmatrix}$$

$$\underline{a} = (a_0, a_1, b_1)^T \; ; \qquad \beta(t) = a_0(t) - a_1(t)\cos\psi - b_1(t)\sin\psi$$

$$p^2 = 1 + \frac{K_\beta}{I_\beta \Omega^2} + \frac{eM_\beta}{I_\beta} + \frac{\gamma K_1}{8}\left(1 - \frac{4}{3}\varepsilon\right)$$

TABLE 4.- COMPARISON OF CHARACTERISTIC ROOTS OF THE REDUCED AND UNREDUCED TPP MODELS AT $\mu = 0.3$

Lock number (γ)	Basic		$\varepsilon = 0.15$	
	Reduced order	Complete	Reduced order	Complete
2	-0.123 ±j 0.0143[a] -3.995	-0.125 ±j 0.005 -0.125 ±j 0.991 -0.125 ±j 1.991	-0.089 ±j 0.105 -7.596	-0.081 ±j 0.104 -0.081 ±j 1.104 -0.081 ±j 2.104
8	-0.399 ±j 0.209 -0.998	-0.513 ±j 0.140 -0.498 ±j 0.843 -0.489 ±j 1.855	-0.308 -0.345 -1.909	-0.325 ±j 0.053 -0.322 ±j 1.052 -0.320 ±j 2.055
16	-0.479 ±j 0.482 -0.563	-1.526 ±j 0.446 -0.659 ±j 0.494 -0.815 ±j 1.290	-0.492 ±j 0.233 -0.985	-0.672 ±j 0.114 -0.639 ±j 0.853 -0.624 ±j 1.889

[a]Normalized with the rotor rotating frequency $\Omega = 31.41$ rad/sec.

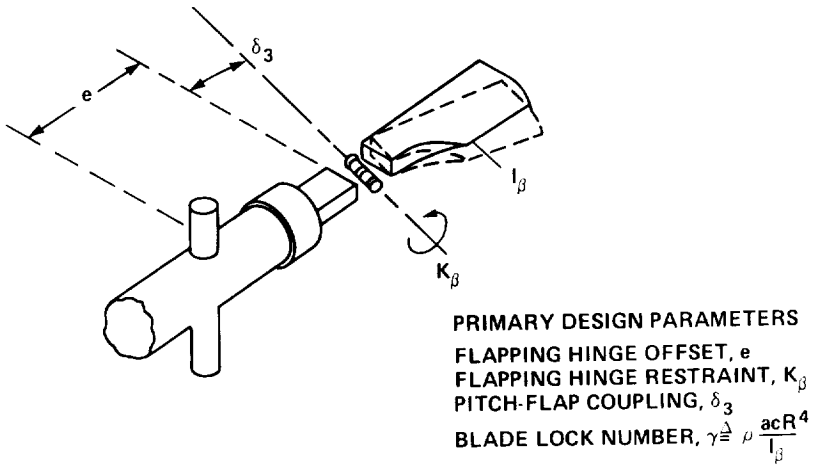

Figure 1.- Main rotor primary design parameters.

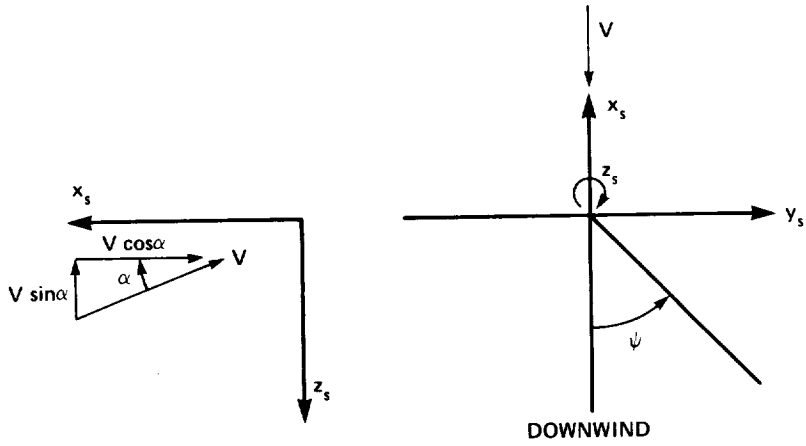

Figure 2.- Coordinate system for the main rotor.

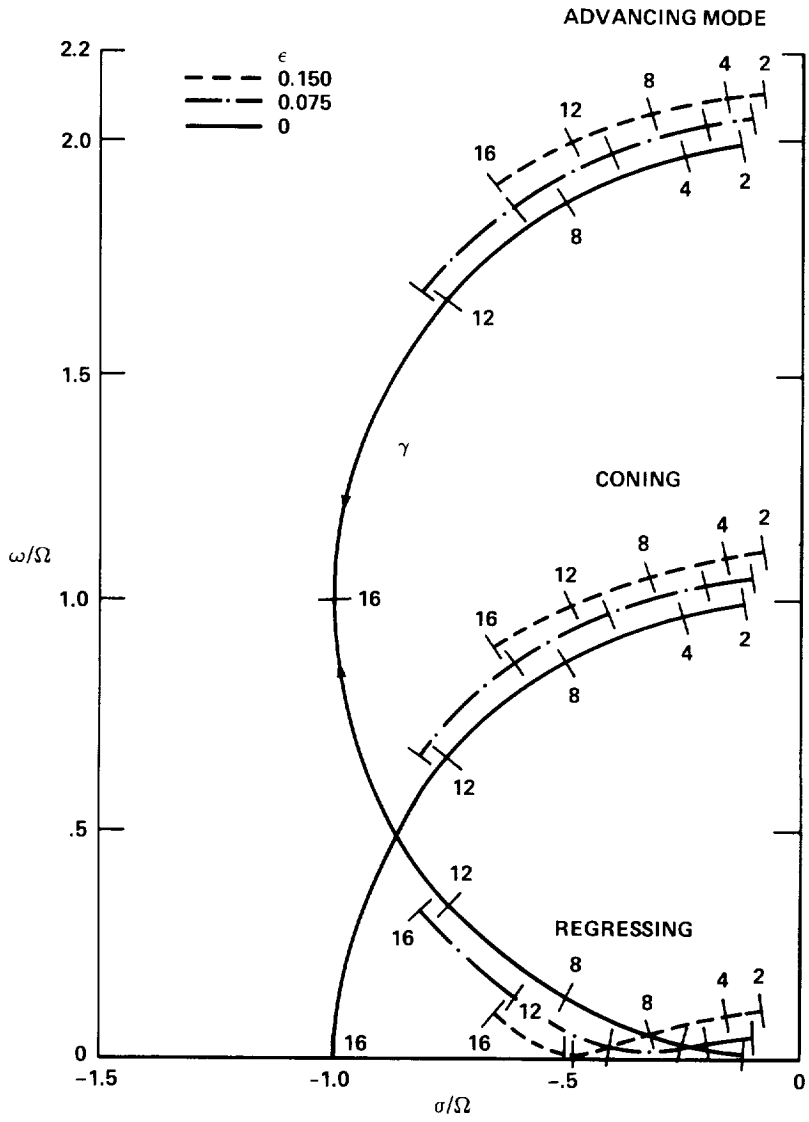

Figure 3.- Effect of hinge offset and Lock number on TPP modes at hover.

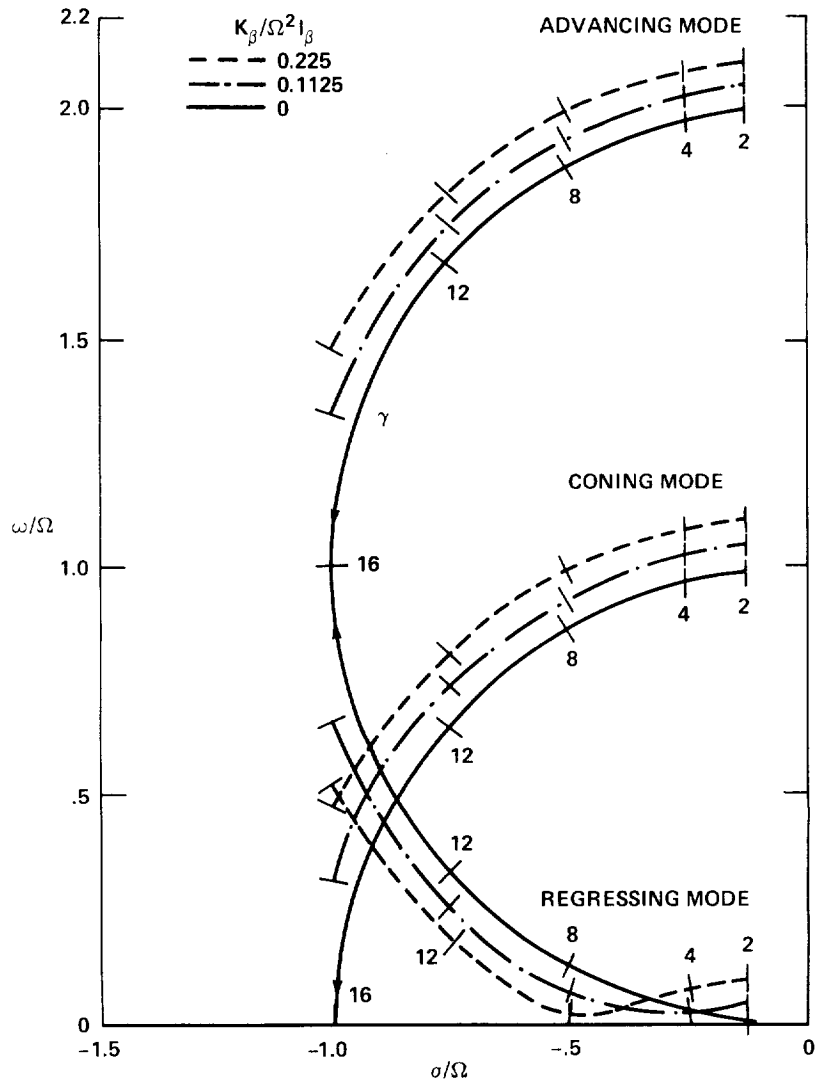

Figure 4.- Effect of hinge restraint and Lock number on TPP modes at hover.

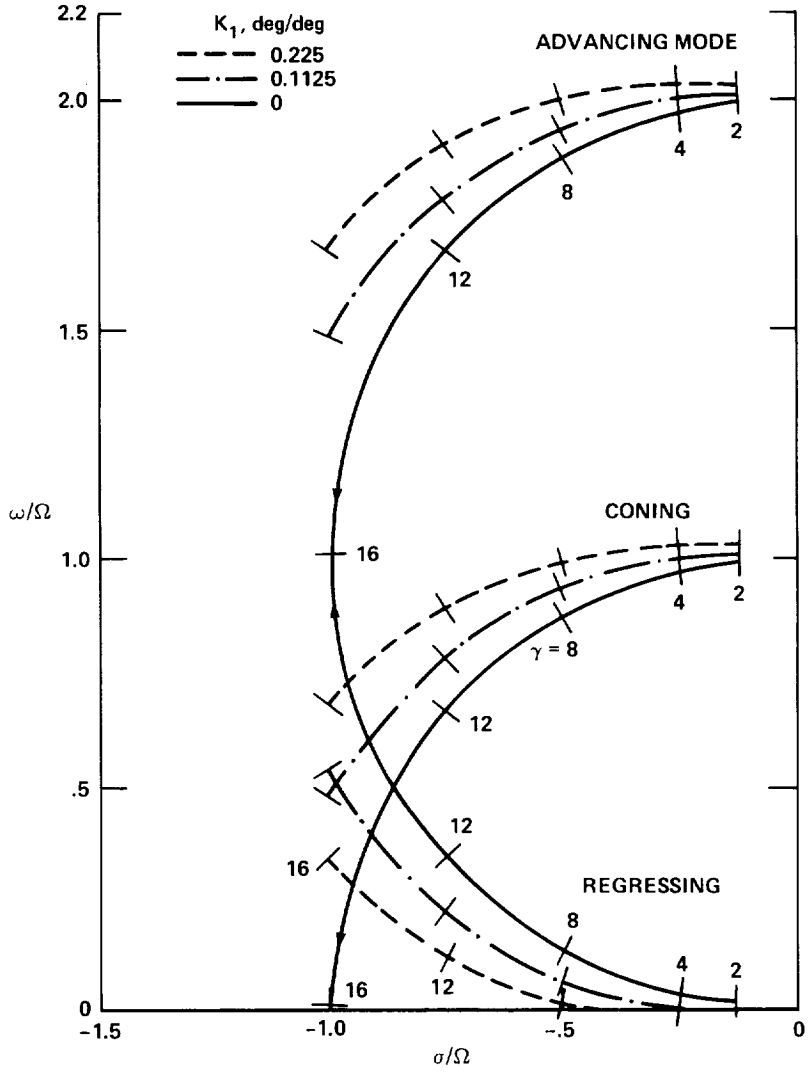

Figure 5.- Effect of pitch-flap coupling and lock number on TPP modes at hover.

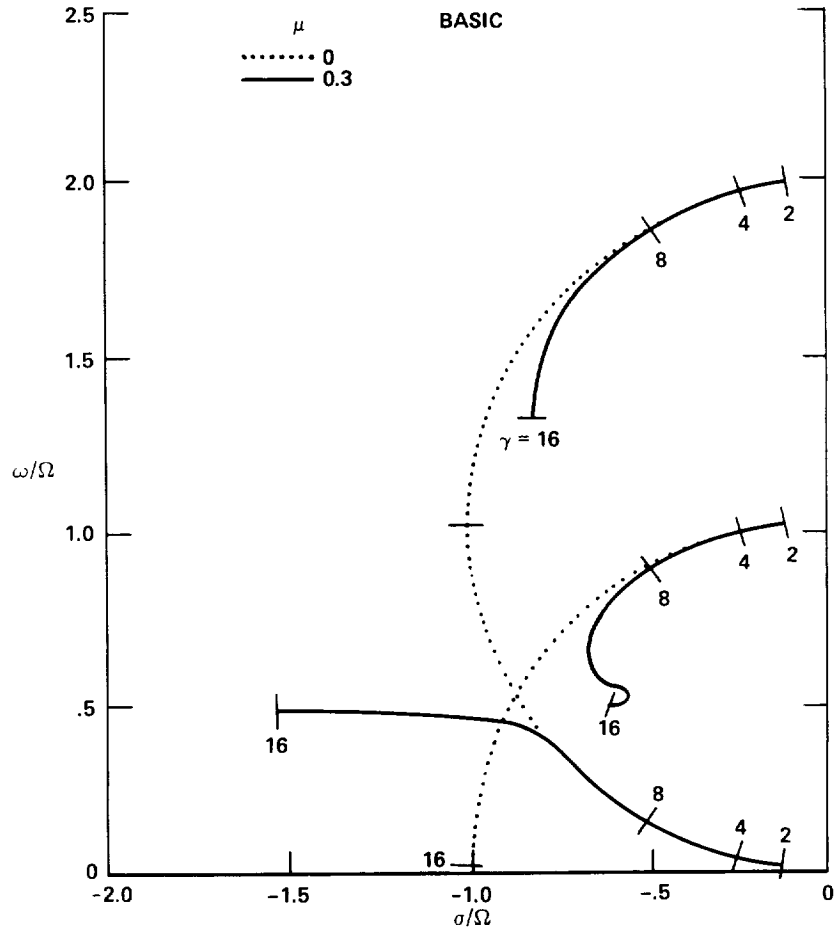

Figure 6.- Effect of advance ratio on the TPP modes, $\varepsilon = K_\beta = K_1 = 0$.

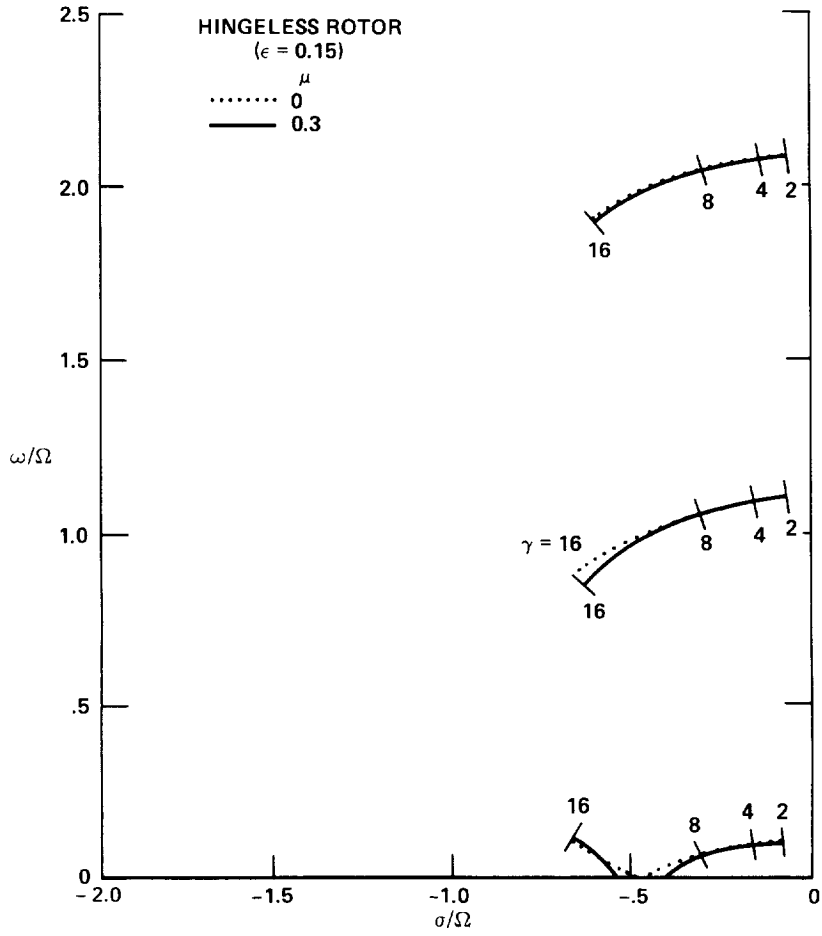

Figure 7.- Effect of advance ratio on the TPP dynamics, $\varepsilon = 0.15$, $K_\beta = K_1 = 0$.

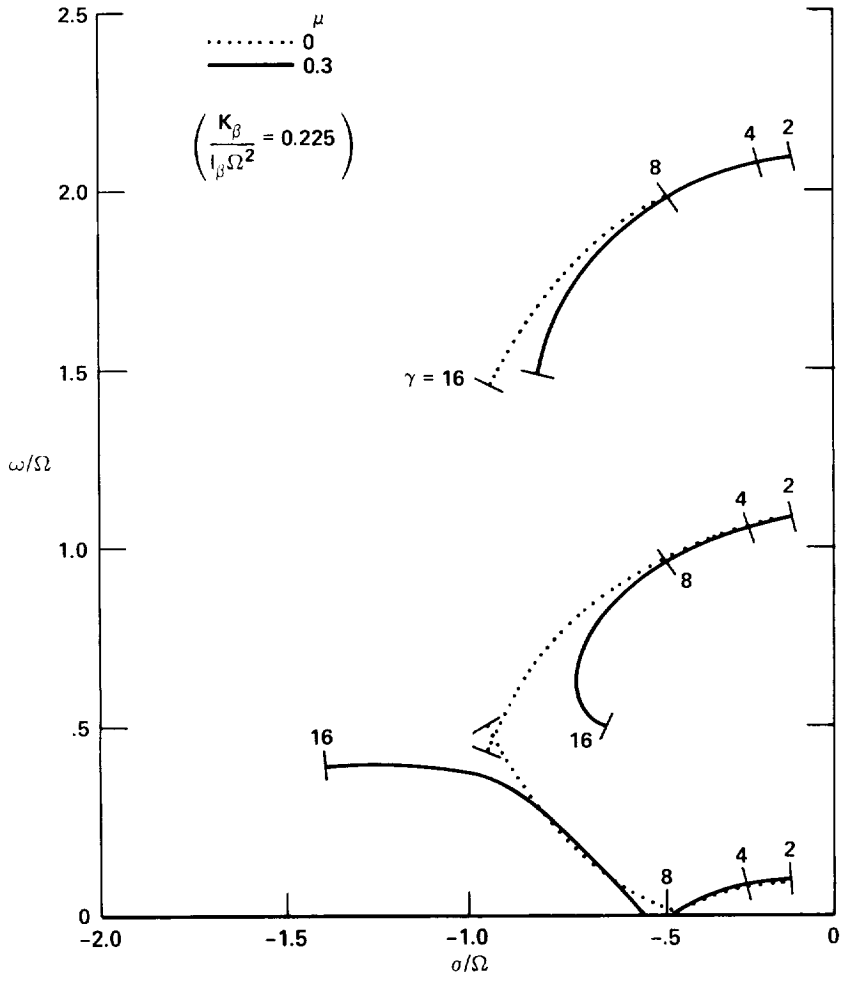

Figure 8.- Effect of advance ratio on the TPP modes, $K_\beta/I_\beta\Omega^2 = 0.225$, $\varepsilon = K_1 = 0$.

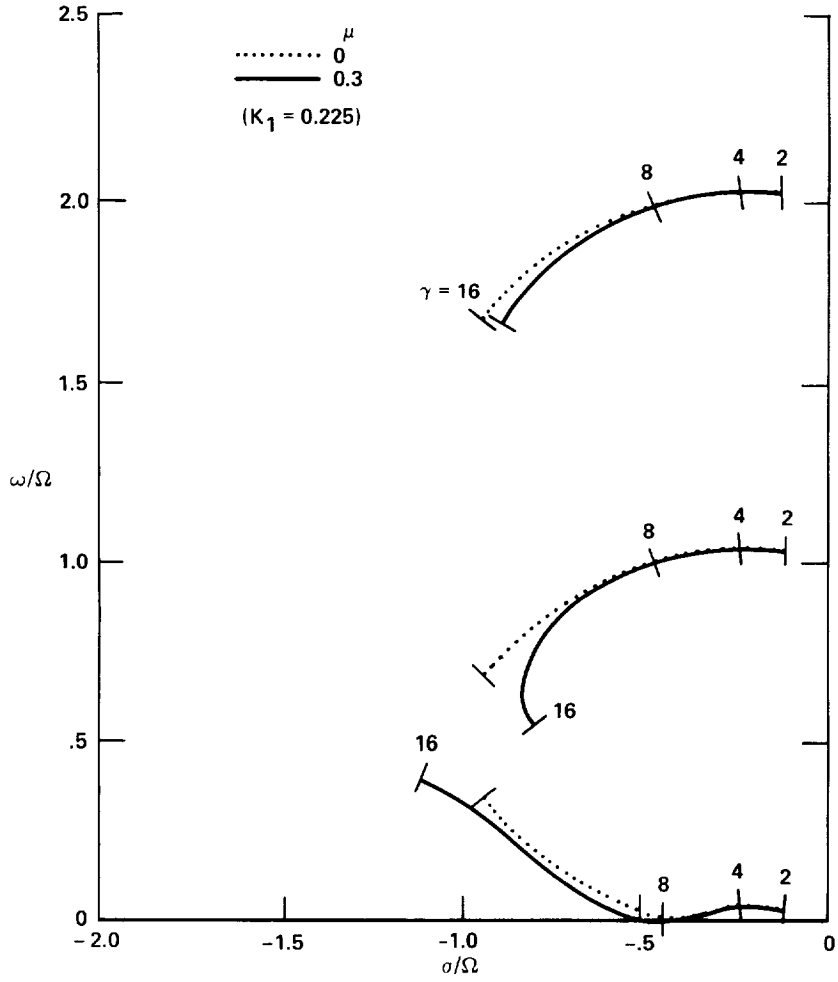

Figure 9.- Effect of advance ratio on the TPP modes, $K_1 = 0.225$, $K_\beta = \varepsilon = 0$.

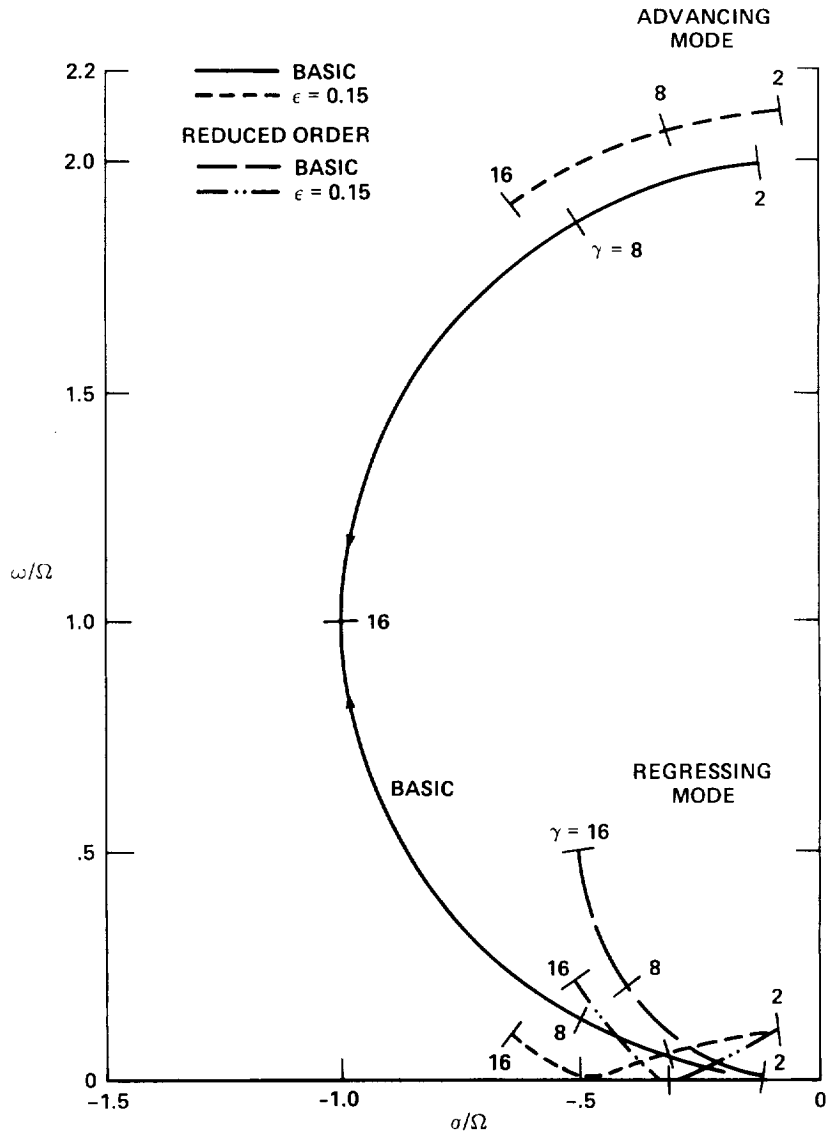

Figure 10.- Comparison of characteristics roots of reduced order and unreduced TPP modes at hover (effect of hinge offset).

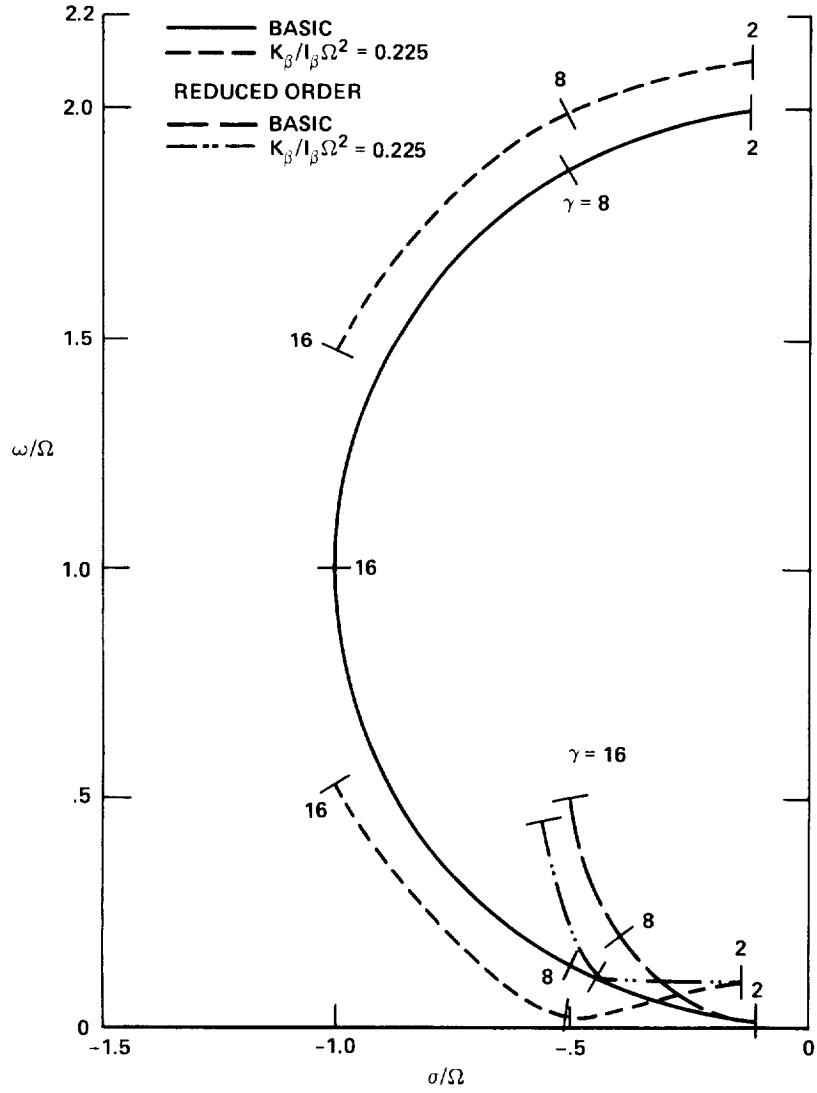

Figure 11.- Comparison of characteristic roots of reduced order and unreduced TPP modes at hover (effect of hinge restraint).

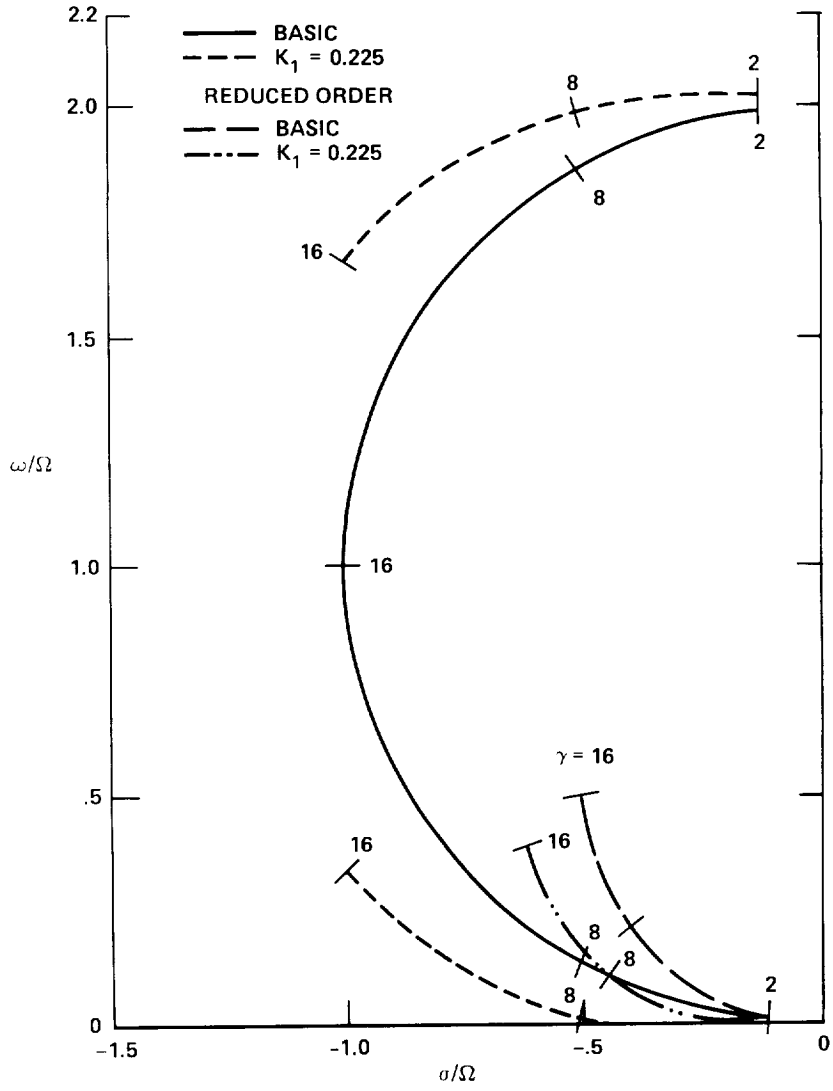

Figure 12.- Comparison of characteristics roots of reduced order and unreduced TPP modes at hover (effect of pitch-flap coupling).

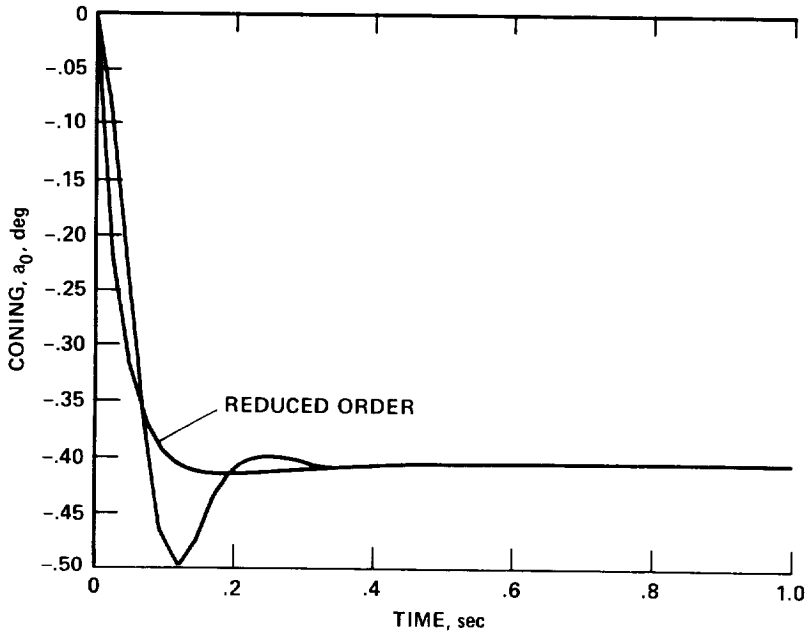

(a) Coning.

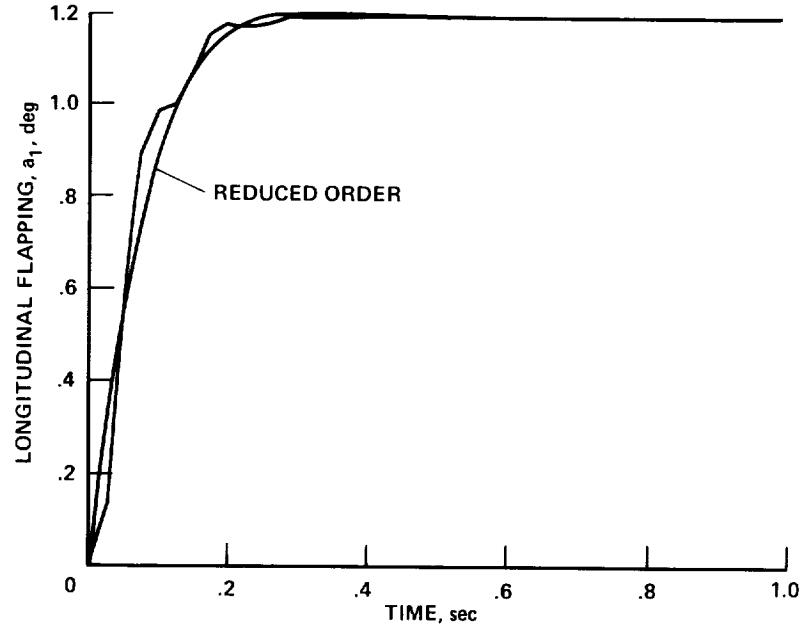

(b) Longitudinal flapping.

Figure 13.- Comparison of responses of the reduced and unreduced order to unit step input in longitudinal cyclic ($K_1 = K_\beta = \varepsilon = 0$, $\mu = 0.3$, $\gamma = 8$).

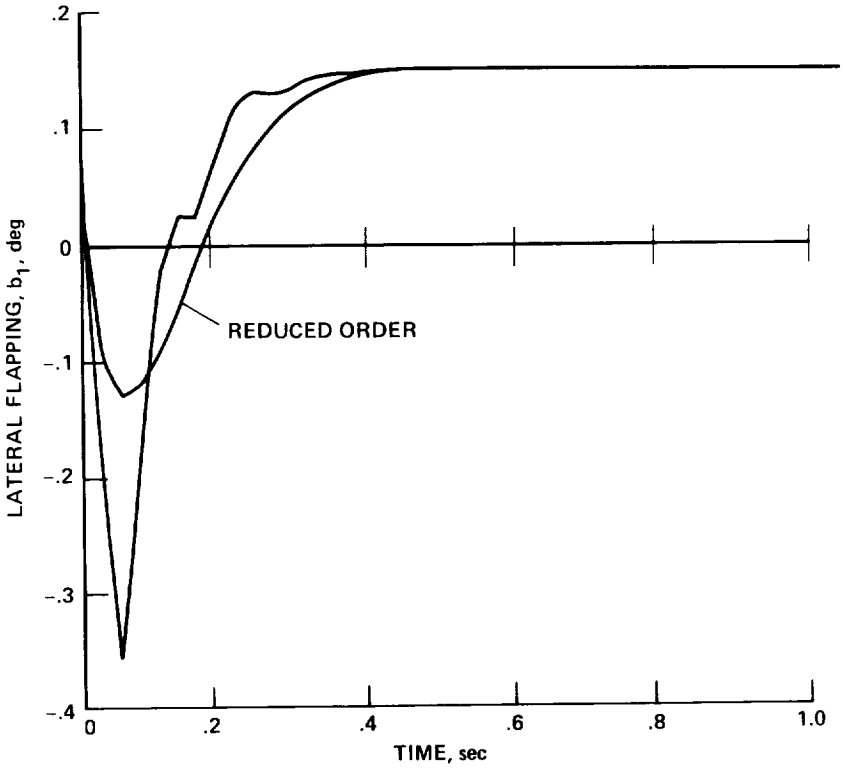

(c) Lateral flapping.

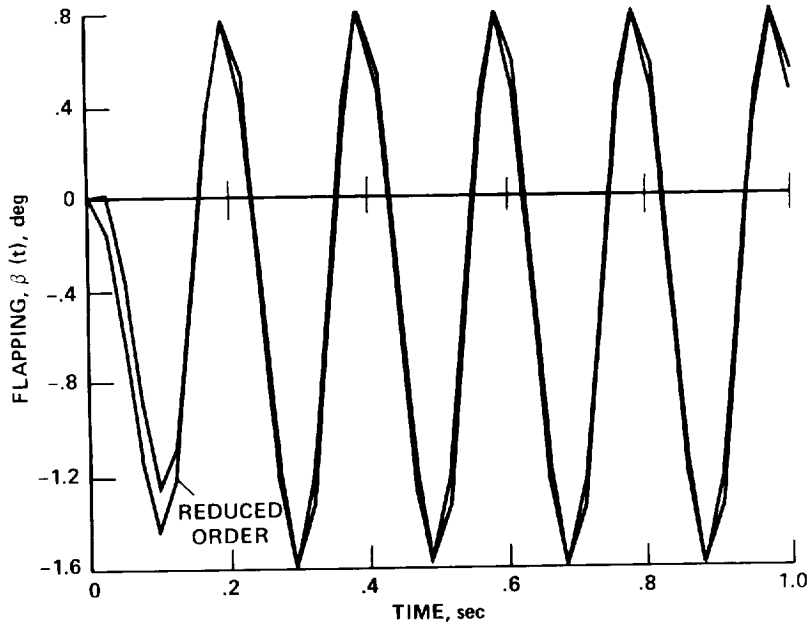

(d) Flapping.

Figure 13.- Concluded.

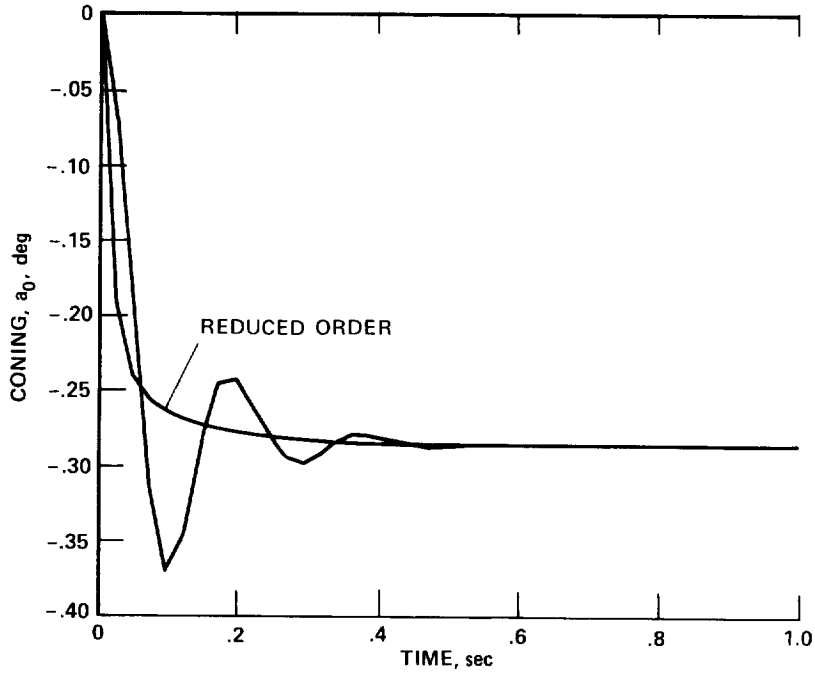

(a) Coning.

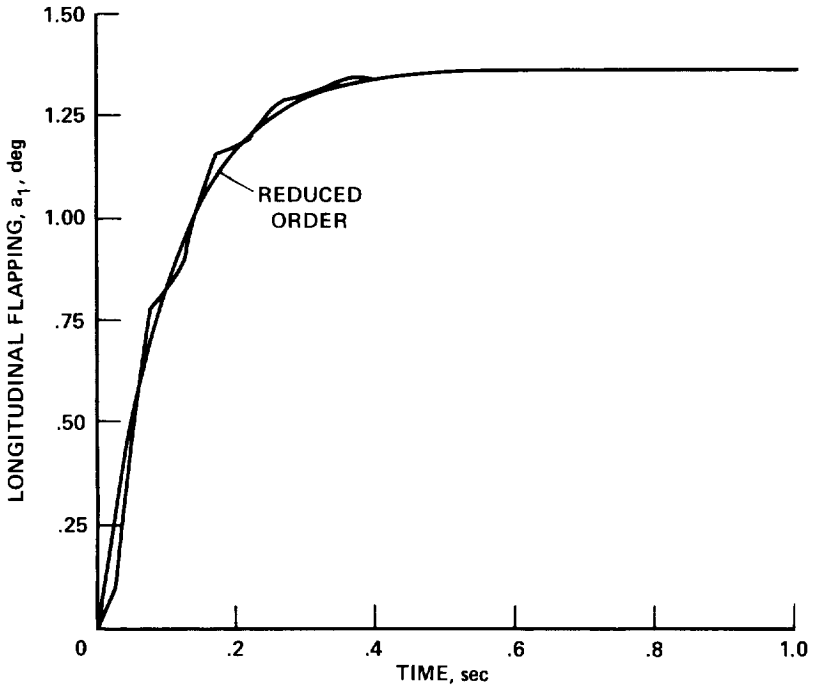

(b) Longitudinal flapping.

Figure 14.- Comparison of responses of the reduced and unreduced order TPP dynamics to unit step input in longitudinal cyclic ($K_1 = K_\beta = 0$, $\varepsilon = 0.15$, $\mu = 0.3$, $\gamma = 8$).

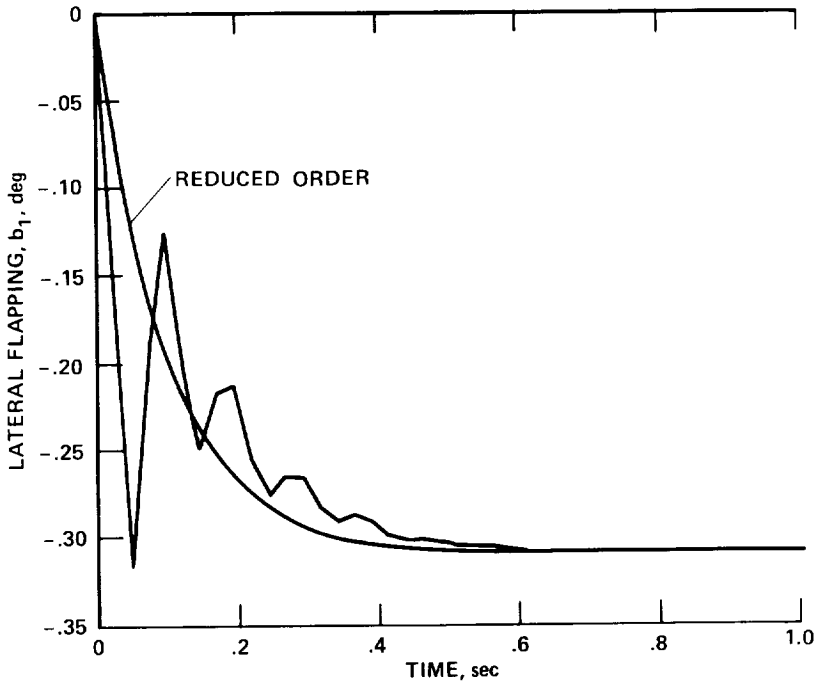

(c) Lateral flapping.

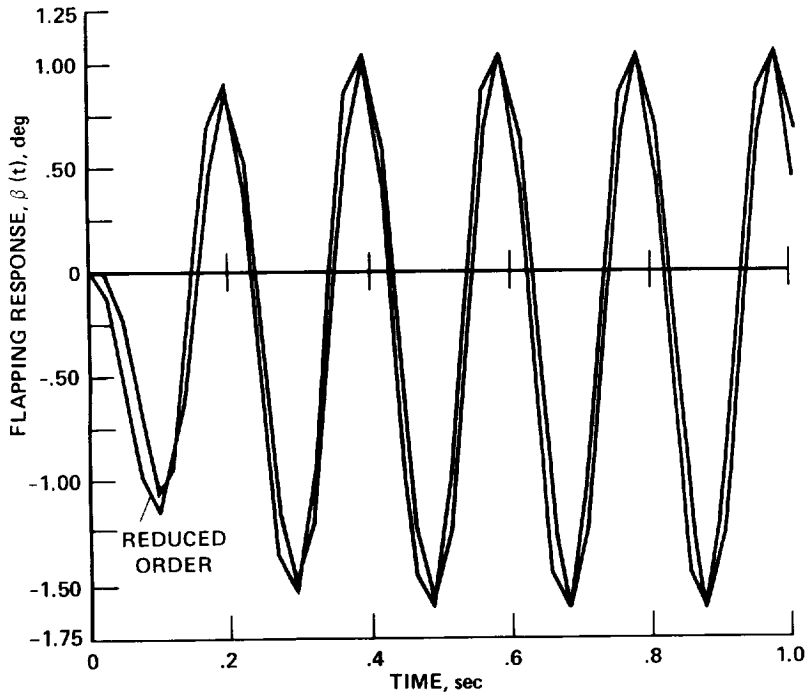

(d) Flapping.

Figure 14.- Concluded.

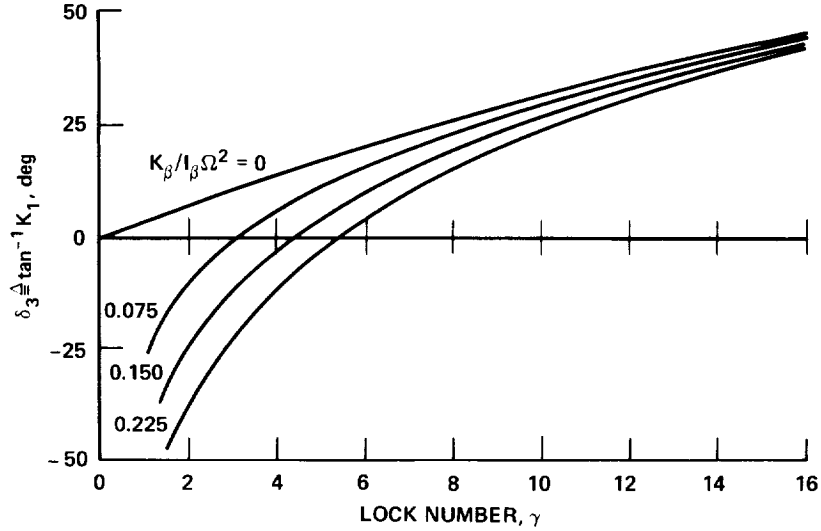

Figure 15.- Pitch-flap coupling required for decoupling flapping due to aircraft angular rate for center-hinged rotor at hover.

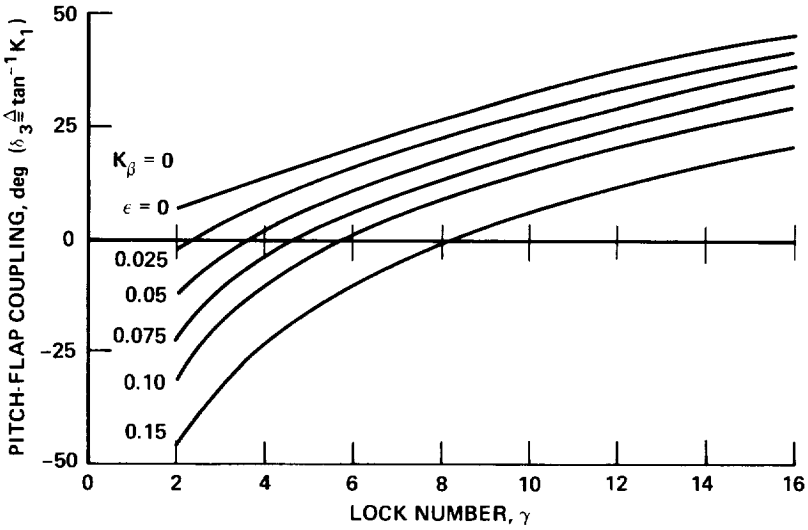

Figure 16.- Pitch-flap coupling required for decoupling flapping due to aircraft angular rate at hover.

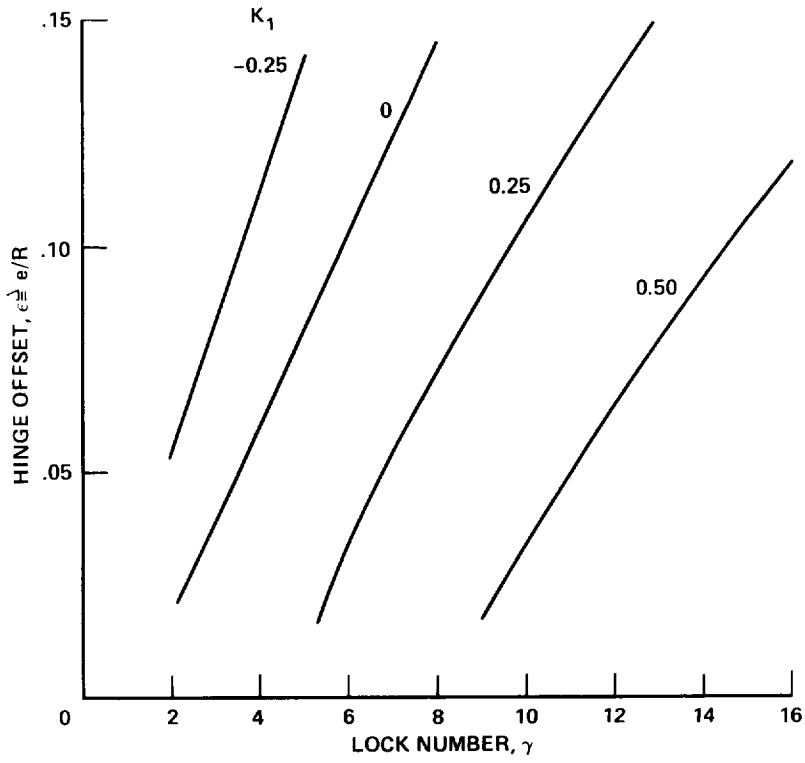

Figure 17.- Hinge offset required to decouple flapping due to aircraft angular rate at hover.

1. Report No.	2. Government Accession No.	3. Recipient's Catalog No.
NASA TP-1431		

4. Title and Subtitle	5. Report Date
EFFECTS OF PRIMARY ROTOR PARAMETERS ON FLAPPING DYNAMICS	January 1980
	6. Performing Organization Code

7. Author(s)	8. Performing Organization Report No.
Robert T. N. Chen	A-7777
	10. Work Unit No.
9. Performing Organization Name and Address	505-10-23
NASA Ames Research Center Moffett Field, Calif. 94035	11. Contract or Grant No.
	13. Type of Report and Period Covered
12. Sponsoring Agency Name and Address	Technical Paper
National Aeronautics and Space Administration Washington, D.C. 20546	14. Sponsoring Agency Code

15. Supplementary Notes

16. Abstract

An analysis has been made to study the effects of flapping dynamics of four main rotor design features that influence the agility, stability, and operational safety of helicopters. The parameters include flapping hinge offset, flapping hinge restraint, pitch-flap coupling, and blade Lock number. First, the flapping equations of motion are derived that explicitly contain the design parameters. The dynamic equations are then developed for the tip-path plane, and the influence of individual and combined variations in the design parameters determined.

The analysis includes a study of the steady-state flapping response with respect to control input and aircraft angular rate which leads to a feedforward control law for control decoupling through cross feed, and a feedback control law to decouple the steady-state flapping response. The condition for achieving perfect decoupling of the flapping response due to aircraft pitch and roll rates without using feedback control is also found for the hover case.

The analysis also indicates that the frequency of the regressing flapping mode of the rotor system can, for some designs, become low enough to require consideration in the assessment of handling characteristics (less than 2 Hz). This occurs for rotors with a large effective hinge offset and with heavy rotor blades.

17. Key Words (Suggested by Author(s))
Flapping dynamics
Tip-path plane
Rotor design parameters
Control decoupling
Feedback control law

18. Distribution Statement
Unlimited

STAR Category - 08

19. Security Classif. (of this report)	20. Security Classif. (of this page)	21. No. of Pages	22. Price*
Unclassified	Unclassified	63	$5.25

*For sale by the National Technical Information Service, Springfield, Virginia 22161

NASA-Langley, 1980